Analysis of Sulfide and Sulfur Oxyanions in Water and Wastewater using Capillary Zone Electrophoresis with Detection by Indirect and Direct UV-Vis Spectrophotometry

By

© Angham H. Saeed

A thesis submitted to the School of Graduate Studies

in partial fulfillment of the requirements for the degree of

Master of Science

Department of Chemistry, Faculty of Science

Memorial University of Newfoundland

July 2017

St. John's Newfoundland

Abstract

Sulfides and sulfur oxyanions, including thiosulfate, sulfate, and polythionates, can impact environmental quality and have negative economic consequences for industrial processes. For example, anaerobic reduction can produce toxic corrosive hydrogen sulfide, and oxidation can lead to environmental acidification accompanied with mobilization of toxic metals. Understanding the chemistry of various systems so that the reductive or oxidative processes can be curtailed requires methods to quantify key sulfur species. Accurate quantitation requires baseline separation and accommodation for co-migrating interferents, such as thiosulfate which co-migrates with chloride, found in abundance in briny waters. A strategy was developed using two capillary zone electrophoresis (CZE) methods, one with direct detection and the other with indirect detection, for speciation analysis of charged sulfur species (sulfate (SO_4^{2-}), thiosulfate ($S_2O_3^{2-}$), tetrathionate ($S_4O_6^{2-}$), sulfite (SO_3^{2-}), and sulfide (S^{2-})) in saline water. Both CZE methods were developed with reverse-polarity in which the anions migrate toward the detector. Hexamethonium hydroxide (HMOH) was added to modify the capillary surface chemistry and reduce EOF toward the inlet, affording methods with shorter time of analysis and better peak resolution. The composition of the background electrolyte (e.g. pH (buffers), flow modifiers, chromophoric probes, etc.) were considered for each method. Also, a chromophoric probe is needed for indirect detection of non-absorbing or weakly absorbing anions. Pyromellitic acid (PMA) was selected because it is non-oxidizing, has high molar absorptivity (high sensitivity), and is a good mobility match for thiosalts. Other factors taken into consideration include capillary length, separation

temperature, potential applied, and use of a stabilizing agent to limit spontaneous oxidation of some of the sulfur-containing compounds.

Acknowledgments

I would like to express my gratitude and appreciation to my supervisor Dr. Christina Bottaro for guiding and supporting me through the learning process of this master thesis. You have set an example of excellence as a researcher, mentor, instructor, and role model.

Furthermore, I would like to thank my committee members, Dr. Kelly Hawboldt and Dr. Penny Morrill for their useful discussions, ideas, and feedback which have been immensely valuable through this process

I am grateful to my colleague Dr. Ali Modir for his help, advice, support, and useful suggestions that have helped me successfully complete my work. My appreciation also goes to all my office colleagues in the Bottaro group. I could not have come this far in my work without everyone's help.

I would also like to thank CCART member, Linda Windsor, for her support in maintaining CE-UV-Vis instruments.

Thanks to my beloved father (Hussain), although your life has ended, your legacy of wisdom, integrity and courage will go on forever. My thanks to my darling husband, Saad, who lost his battle with cancer. Your memory is engraved in me and encourages me to continue on my way.

I would like to thank my loved ones, my amazing children (Ali Alwaznee and Ghena Alwaznee) who have supported and have constantly encouraged me throughout my journey, and you both have given me the passion to me to continue my life.

I would like to extend my heartfelt gratitude and appreciation to my mother Fadheelah, sisters (Ahlam, Anaam, and Shaymaa), and brothers (Ali, Mohammed, and Ahmed). In addition, special thanks to my nephews and nieces. You are all the salt of the earth, and undoubtedly, I could not have done this without you.

Finally, I would like to thank the Department of Chemistry and School of Graduate Studies at Memorial University of Newfoundland, as well as Suncor Energy, especially Philip Stemler, and Mitacs for their financial and technical support.

Table of Contents

List of Figures

List of Tables

List of Abbreviations

SRB	sulfate reducing bacteria
TSR	thermochemical sulfate reduction
PS	polysulfides
BGE	background electrolyte
IC	ion chromatography
CE	capillary electrophoresis
CEC	capillary electrochromatography
CGE	capillary gel electrophoresis
CIEF	capillary isoelectric focusing
CITP	capillary isotachophoresis
MEKC	micellar electrokinetic chromatography
CTAB	cetyltrimethylammonium bromide
CZE	capillary zone electrophoresis
HPLC	high pressure liquid chromatography
E	electric field
EOF	electroosmotic flow
μ_{ep}	electrophoretic mobility
μ_{eo}	electroosmotic mobility
μ_{app}	apparent electrophoretic mobility
v	migration velocity
V	applied voltage

L	length of the capillary
q	net charge of particle
r	radius
η	viscosity
i.d.	internal diameter
o.d.	outer diameter
LOD	limit of detection
UV	ultraviolet
UV-Vis	ultraviolet-visible
λ_{max}	maximum absorption wavelengths
DAD	diode array detector
LIF	laser-induced fluorescence
RI	refractive index
DTPA	diethylenetriaminepentacetic acid
PMA	pyromellitic acid (1, 2, 4, 5- tetracarboxylic acid)
HMOH	hexamethanium hydroxide
TMAOH	tetramethylammonium hydroxide
CTAB	hexadecyltrimethylammonium bromide
BIS-TRIS	BIS [2- Hydroxyethylaminotris[hydroxymethyl]methane]
TEA	triethanolamine
Ox	oxidant
Red	reductant
DC	direct current

Redox	oxidation and reduction reactions
E^o	standard oxidation-reduction potential

Chapter 1. Introduction and Overview of Thiosalts Chemistry and Analytical Approaches for Their Analysis

1.1 General Introduction

Sulfur-containing species present in the environment and in onshore and offshore oil processing systems (e.g., produced water) play an important role in damaging the environment.[1,2] Sulfur-oxygen species are produced as a result of oxidative processes in natural sulfur-rich aqueous environments or during the crushing, milling and floatation of sulfidic ores. Sulfur is found with a wide range of oxidation states including sulfide and reduced organic sulfur (2-), elemental sulfur (0) and sulfate (6+).[3] Thiosalts ($S_xO_y^{2-}$), sulfur oxyanions containing S-S bonds, and polysulfide (S_n^{2-}) are important intermediate species implicated in redox transformations of sulfur compounds, metabolism of sulfur-oxidizing and sulfur reducing microorganisms. Sulfur reduction–oxidation reactions generate a sulfur cycle (Figure 1.1).[4] Sulfur-oxygen species can be reduced to the toxic and corrosive hydrogen sulfide (H_2S) in anaerobic environments as found in onshore or offshore oil and gas reservoirs and process streams.[2,5,6] Hydrogen sulfide is a malodorous and toxic gas; it is extremely harmful to human health to life second only to carbon monoxide as a cause of inhalation deaths, and severely lowers air quality. Moreover, oxidation of sulfide to sulfur dioxide and sulfite in the presence of sulfur oxyanions can lead to acidification of the environment (pH depression) and mobilization of toxic metals.[7]

Reservoir souring is a widespread phenomenon occurring across the petroleum industry, and is due to the increase of hydrogen sulfide, especially after secondary

recovery where sea water is injected into the reservoir to force oil to the surface.[2,8] Hydrogen sulfide and its ionization products, bisulfide (HS^-) and sulfide (S^{2-}), may be either indigenous to oil and gas reservoirs or originating from the reduction of sulfate by biotic or abiotic mechanism.[9,10,11,12] Sulfate reducing bacteria (SRB) are considered the primary biogenic reservoir souring mechanism. On the other hand, thermochemical sulfate reduction (TSR), thermal hydrolysis of organic sulfur compounds, hydrolysis of metal sulfides, and desorption of H_2S from the aqueous phase, with a decrease in reservoir pressure, are among the non-biogenic mechanisms.[11,13] Souring causes many operational problems, such as an increase in corrosion, plugged oil field, and increased costs of refinement.[14,15,16] Hence, the sulfur cycle can ultimately lead to higher operational costs for industrial processes whether from the cost of treatment or from the refit of damaged equipment.[17]

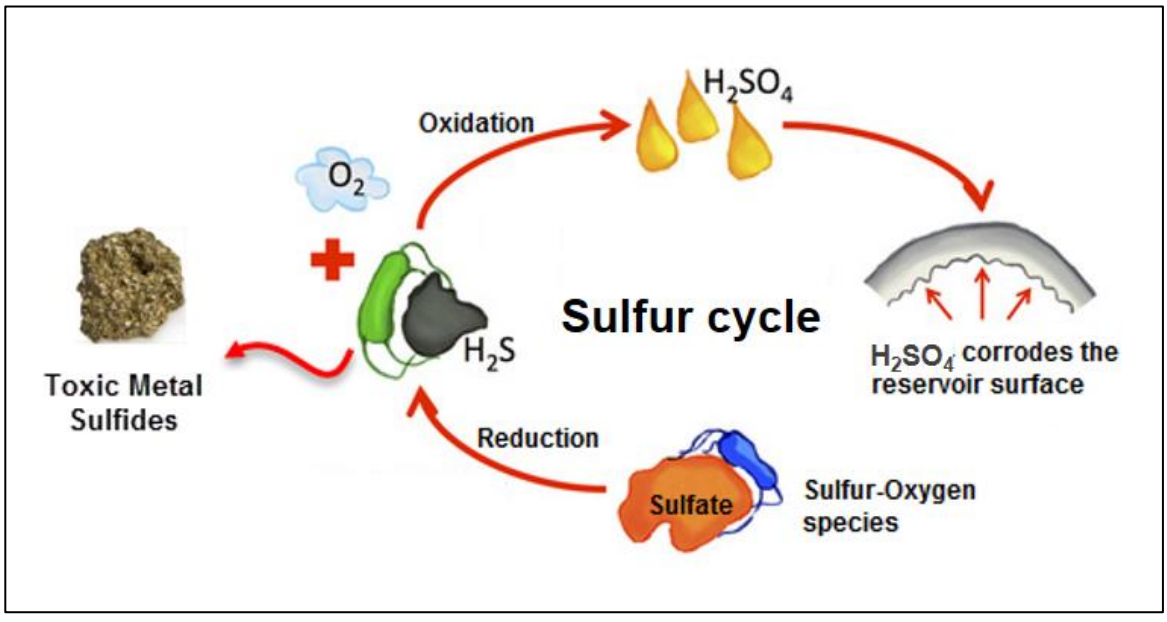

Figure 1.1 Sulfur cycle. [17]

The structures of the most common sulfur species are shown in Figure 1.2 including polythionates, which are sulfur-based molecules where a sulfur chain is terminated at both ends by an SO_3 group.[18,19,20]

Understanding the chemistry and behaviour of sulfur species as contaminants in process infrastructure is necessary to reduce souring and this requires the understanding of the mechanisms causing the reservoir souring and methods to reliably measure the target species.

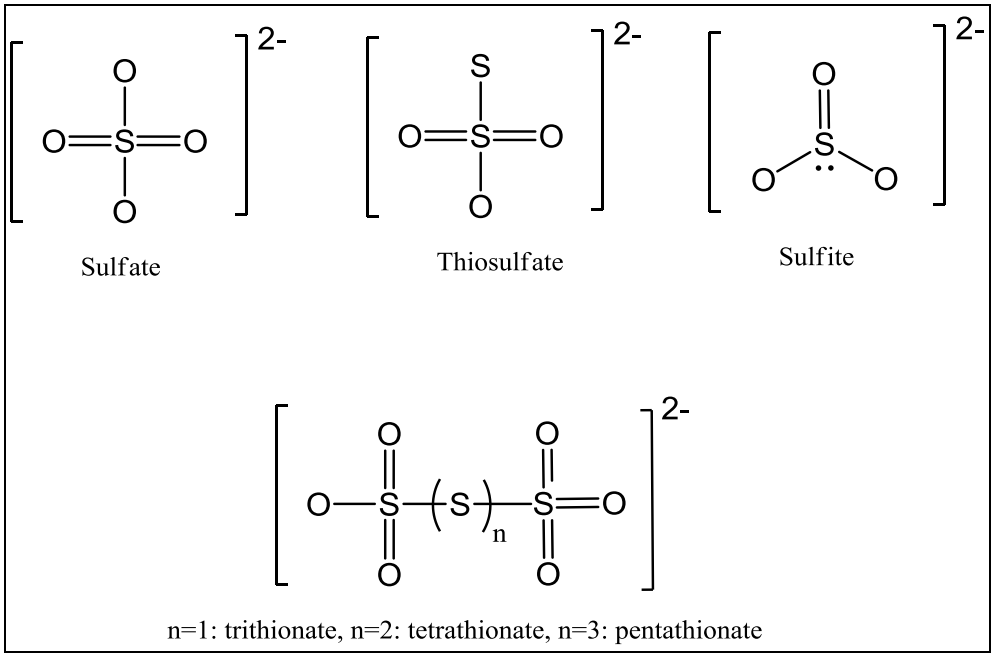

Figure 1.1. Structures of key sulfur species.

1.2 Reservoir Souring Generation

1.2.1 Microbial Sulfate Reduction

Hydrogen sulfide may be generated naturally in oil and gas reservoirs or catalyzed by sulfate-reducing bacteria (SRB) at low temperatures. SRB live naturally in the shallow depths of the reservoirs at low temperatures (below 80 °C) or can be injected into the reservoir with the seawater used for oil and gas processing. In the environments lacking oxygen, these microorganisms obtain energy for growth through oxidation of organic nutrients (e.g., low-chain fatty acids (VFA) such as acetate, propionate, and butyrate) with the simultaneous reduction of sulfate to sulfide in a suitable temperature regime (typically ranging from 35 to 95 °C) and the presence of nutrients (e.g., phosphorus, nitrogen, and trace elements).[21] SRB are considered the primary source of hydrogen sulfide in many oil and gas reservoirs as the injection of water contains a high level of sulfate (25-30 mM).[2,8,22] Approximately 70% of reservoir souring has taken place in fields under seawater flooding where seawater is injected into an oil field to increase oil recovery from an existing reservoir.[21]

Limiting SRB growth reduces microbial production of sulfide. SRB growth can be limited naturally in high salinity media and at high reservoir temperatures (>100 °C) or by adding chemical additives such as oxidizers, biocides, and nitrate/nitrite.[8,21,22,23]

1.2.2 Thermochemical Sulfate Reduction (Abiotic Sulfate Reduction)

Hydrogen sulfide can be a product of thermochemical sulfate reduction (TSR) of aqueous sulfate mediated by a variety of organic compounds such as alcohols, polar aromatic hydrocarbons, and saturated hydrocarbons, at temperatures above 80 °C.[24,25,26] TSR

occurs at a slower rate than SRB even though it appears to be a geologically relatively faster process under favorable circumstances. However, TSR is still a significant source of H_2S.[9,10] Gypsum ($CaSO_4 \cdot 2H_2O$) and/or anhydrite ($CaSO_4$) dissolution, seawater, and evaporitic brines are the sources of sulfate that results in a high concentration of H_2S in TSR.[9] The anhydrite reaction with hydrocarbons form H_2S in addition to producing other by-products such as elemental sulfur, carbonate minerals (calcite, $CaCO_3$), carbon dioxide, and water as in the reaction below:[9,10,24,27,28]

$$\text{anhydrite} + \text{hydrocarbons} \longrightarrow CaCO_3 + H_2S + H_2O + S^* + CO_2^* \qquad (1.1)$$

*Elemental sulfur and carbon dioxide may be produced in some, but not all, instances.

The reduction of sulfate (S^{6+}) to lower valence states, such as S^o/polysulfides, thiosulfate, and sulfite, depends on the types of reactive organic compounds present and the pH of the system. However, these intermediate compounds are usually unstable and are further reduced to sulfide.[10,26,28]

Crude oil and its source, kerogen, can contribute in the production of small amounts of H_2S along with HS^-, polysulfides (PS), gas, and gas condensate during TSR.[10]

$$\text{Crude Oil} \longrightarrow \text{Light Crude Oil} + H_2S + PS + CH_4 \qquad (1.2)$$

1.2.3 Hydrolysis of Metal Sulfides

Hydrolysis of metal sulfides associated with oil/rock formation is considered a source of the observed geological hydrogen sulfide. The common metal sulfides accounting for almost all of the sulfur emissions are iron, copper, nickel, zinc, and lead.[29,30] These metal sulfides are reactive under various conditions: 1) in an oxidizing environment sulfate ions

are generated in solution; this process is partially dependent on oxidizing potential and pH; 2) in strongly acidic solutions H_2S is generated and metal ions released. Equations 1.3, and 1.4 show metal sulfide (MS) reactivity with the environment, where O and R are oxidized and reduced states of some appropriate redox couple, or for electrochemical experiments.[30,31]

a) Oxidation:

$$MS + 4H_2O + xO \longrightarrow M^{2+} + SO_4^{2-} + 8H^+ + xR \qquad (1.3)$$

b) Acid decomposition:

$$MS + 2HCl \longrightarrow MCl_2 + H_2S \qquad (1.4)$$

1.2.4 Desorption of Hydrogen Sulfide from Aqueous Phase

Releasing H_2S from fluids with pressure reduction during oil and gas operations is another potential mechanism for reservoir souring. Hydrogen sulfide solubility in water decreases with increasing temperature, decreasing the pressure, and at a pH lower than 7.[32]

1.2.5 Thermal Hydrolysis of Organic Sulfur Compounds

The reactivity of sulfur compounds during thermal recovery of heavy oil has a negative effect on oil and gas operations and on the environment due to the production of H_2S and other inorganic sulfur compounds (e.g., SO_2). Hydrogen sulfide and other gases can be produced from hydrothermolysis reactions between oil and saturated steam at

temperatures below 240 °C. Above this temperature, a similar gas can form from thermolysis (thermal cracking) reactions. Thiophene (aromatic organosulfur compounds) and tetrahydrothiophene (saturated cyclic organic sulfides) are major contributors to H_2S production during thermal processing. Time of heating and pH are the most important parameters controlling H_2S production from thermal decomposition of sulfur-containing components of oil.[13] For example, the hydrolysis rate of thiophene ($C_4H_3S^-$) is faster in an acidic system than in a neutral media, which is probably due to the protons present and also the sulfate anions, which act as an oxidizing agent.[6] Sulfur element hydrolysis can yield H_2S in both alkaline and acidic solutions at high temperatures.[20]

1.3 Generation of Sulfur Oxyanions Species

Sulfur has a wide range of oxidation states due to its redox capability by means of sulfur-oxidizing and sulfur-reducing microorganism metabolism. [3,4,8,19] The generation of sulfur oxyanions and their behaviour are affected by many factors including the sulfur content of the ore, pH, reservoir water temperature, residence time in the reservoir, and the presence of air and SO_2 gas.[13,19,20,33] Sulfur oxyanion species, which are called thiosalts ($S_xO_y^{2-}$) containing S-S bonds, are key intermediates in oxidation- reduction reactions. For example, H_2S and metal sulfides can be oxidized to sulfate, sulfite , sulfur dioxide, thiosalts, and elemental sulfur.[32,34] Sulfate can be reduced to sulfide by sulfate reducing microorganism. Thiosulfate decomposes to elemental sulfur, H_2S, and polythionic acids $H_2S_nO_6$ (Wackenroeders solutions) in acidic media, with subsequent volatilization of H_2S and SO_2. Hydrogen sulfide also reacts with SO_2 in a water solution leading to complex mixtures of sulfur-oxygen species in a highly diluted aqueous solution ($H_2S_nO_6$).[3,34,35,36]

Polythionates are sulfur-based molecules in which a sulfur chain is terminated at both ends by -SO_3 groups. Sulfur oxygen species chain lengths are generally governed by the following equilibrium:[19,33]

$$S_xO_6^{2-} + S_2O_3^{2-} \rightleftharpoons S_{x+1}O_6^{2-} + SO_3^{2-} \quad (1.5)$$

Therefore, complex physical and chemical processes can take place in oil and gas systems, including precipitation of heavy metals and various redox reactions.[3,35,34,36] These compounds play an important role in nature as they exhibit toxicity and affect the behavior of metal ions in the environment. According to aquatic environmental toxicity, thiosulfate ($S_2O_3^{2-}$), trithionate ($S_3O_6^{2-}$), and tetrathionate ($S_4O_6^{2-}$) are the most important species amongst the thiosalts, and are a major concern to industry.[34]

1.4 Analytical Methods for Detection of Sulfur Species

Understanding the chemistry and behavior of sulfur species as contaminants in process infrastructure requires the development of analytical methods. The goal of new methods should be to improve and simplify current techniques in terms of sensitivity, selectivity, reproducibility and robustness, or to make a modification for application in different media. Many analysis techniques have been developed for the determination of sulfur species as inorganic anions in environmental matrices. Modern methods have been based on ion chromatography and capillary electrophoresis, since conventional methods are quite time-consuming and difficult to employ in the analysis of sulfur anions in very complex matrices.[4,37,38,36,39]

1.4.1 Chromatographic Techniques (Ion Chromatography (IC))

Ion chromatography (IC) with various detection techniques has been extensively used for the speciation of sulfur compounds in an aqueous phase in environment matrices.[36,40] IC was the first viable analytical method used for the simultaneous determination of inorganic anions at trace levels with good reliability.[40] IC employs columns packed with either anion or cation exchange resins combined with a suitable mode of detection, such as spectrophotometric and electrochemical detectors. IC development for sulfur anions began with the awareness of the environmental impact on sulfur species, particularly, the thiosalts.[41,42]

Despite IC having a good sensitivity, there are some limitations including the high cost of consumables. In particular, the columns can be damaged by matrix components which requires careful sample pre-treatment. Additionally, IC exhibits only moderate separation efficiency and speed. These limitations have encouraged the use of other techniques, such as capillary electrophoresis (CE).[38,43,44,45]

1.4.2 Capillary Electrophoresis

Capillary electrophoresis (CE) has emerged as a versatile and robust separation technique for speciation analysis of environmental and biological molecules, inorganic ions and a variety of other compounds. The term ‘electrophoresis’ was created by Michaelis in 1909 after studying the migration of charged particles in an electric field. Electrophoresis was used for the first time as a technique to separate mixtures in 1937 by Arne Tiselius after applying an electric field to separate the components of a mixture of proteins.[46,47,48] CE was introduced in the1960s as a separation technique for ions based on their size to

charge ratio.[44] CE has grown to include several modes including capillary zone electrophoresis (CZE), capillary isoelectric focusing (CIEF), capillary gel electrophoresis (CGE), capillary isotachophoresis (CITP), micellar electrokinetic chromatography (MEKC) and capillary electro-chromatography (CEC).[48] CE is considered as an alternative to traditional methods due to its high separation efficiency and speed, low cost of consumables as well as better tolerances for sample matrices with high ionic strength. Additionally, CE is green due to its low injection volume of sample and background electrolyte (nL range) leading the generation of a low amount of waste.

The successful application of the separation techniques requires that (i) the reaction of sulfur species should be slow compared to the separation process; (ii) there is no change in the reaction mechanism by the pH and other conditions used in the separation, that is, the reaction should occur within the capillary column in the same manner as in a solution; and (iii) concentrations of relevant species in the reaction solution are measurable within the linear range of detection. Therefore, CE is well suited for the analysis of unstable sulfur- containing species as CE is rapid and minimizes sulfur species reaction during separation. Furthermore, CE provides a better correlation between the analytical results and characteristics of the source, particularly with regard to industrial applications of the technique.[49]

CZE separation occurs due to the differences in mobilities of analyte ions in an electrolyte solution under the influence of an applied electric field. Mobility is a function of the hydrodynamic radius and charge of the analytes. The mobility of chemical compounds inside the capillary is controlled by two actions: the electroosmotic flow and the electrophoretic migration, which is an intrinsic property of the ion; both actions are a

result of the applied electric field across the capillary. Electrophoretic mobility (μ_{ep}) is the constant proportionality of the migration velocity, v of an analyte in an electric field (E) . Electric field strength is proportional to the applied voltage and inversely proportional to the capillary length. Therefore, applying higher voltages are needed with an increase in the capillary length:[48]

$$v = \mu_{ep}E = \mu_{ep}\frac{V}{L} \quad (1.1)$$

where v is the migration velocity (cm s^{-1}), μ_{ep} is the electrophoretic mobility (cm^{-2} $V^{-1}s^{-1}$), V is the applied voltage (V) and L is the length of the capillary (cm). The μ_{ep} is an inherent property of the charged analyte and is given by:

$$\mu_{ep} = \frac{q}{6\pi\eta r} \quad (1.2)$$

Electrophoretic mobility (μ_{ep}) is proportional to the net charge of the particle (q), and inversely proportional to its radius (r) and environment viscosity (η). This equation proves that electrophoretic mobility is greater for small particles with a big charge, and lower for larger particles with a small charge, while it is equal to zero for neutral particles because q= 0. Note that buffer viscosity is influenced by a change in temperature which causes changes in the electrophoretic mobility of particles.

1.4.2.1 Electroosmotic Flow (EOF)

Electroosmotic flow (EOF) is a bulk flow induced by the difference in potential applied at the ends of a fluid filled capillary. It requires ionization of functional groups present on the inner capillary surface. Silanol (Si-OH) groups of the internal wall of a fused-silica

capillary are deprotonated leaving negatively charged groups (Si-O-) at the surface depending on the pH of the electrolyte (Eq. 1.11):[48]

$$\text{Si-OH} \rightleftharpoons \text{Si-O}^- + \text{H}^+ \qquad (1.6)$$

In aqueous conditions with pH > 3, silanol groups are dissociated and lead to the formation of an excess of negative charge on the silica narrow bore capillary surface. Counter ions (cations, in most cases) in the electrolyte are tightly adsorbed onto the surface of the capillary to compensate for the negatively charged wall which is formed (Figure 1.3). These attractive forces result in an electric double layer on the border phases of the electrolyte/capillary wall and create a potential (zeta potential) difference close to the capillary wall. A diffusion layer is also formed as there is still a net charge near the surface. The diffuse layer is a layer of solvate ions from the bulk solution weakly bound near the surface of the capillary. Diffusion layer ions are only mobile during the application of an electric field to the capillary. The excess of cations in the diffuse layer are attracted toward the cathode and the flow profile results in a flat profile, as opposed to the parabolic profile for pressure driven chromatographic techniques with laminar flow such as high pressure liquid chromatography (HPLC) (Figure 1.4). Electroosmotic flow can be modified, reversed, or eliminated by covalent or dynamic capillary wall modifications using surfactants or neutral or ionized polymers.

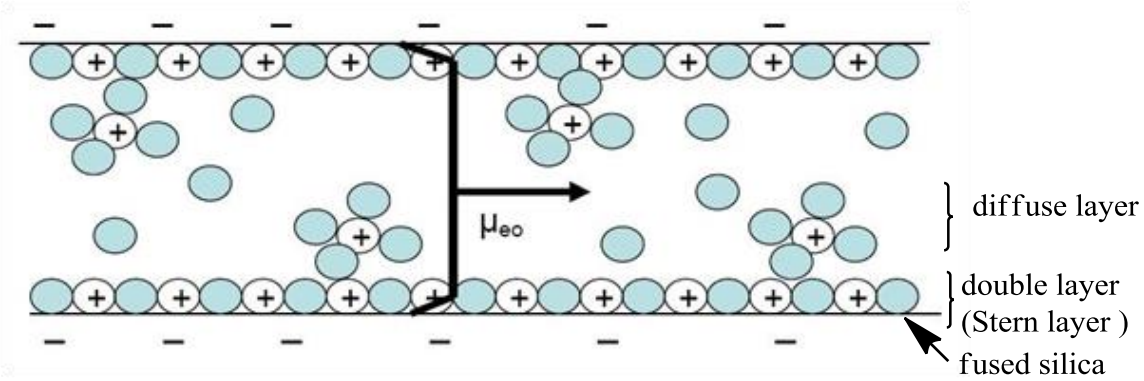

Figure 1.3. Diagram of creation of double electric layer with flat flow profiles of electroosmotic flow.

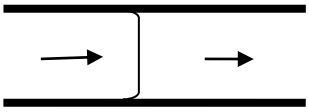

Figure 1.4. Profiles of electroosmotic and laminar flow (such as in HPLC).

1.4.2.2 Mechanism of Electrophoretic Separation

In the presence of the negative charge on the internal surface of the capillary (unmodified capillary), electroosmotic flow moves from the anode to the cathode (positive polarity), where the detector is usually located. All species, including cations, neutrals and anions, will migrate in the presence of the EOF. In positive polarity, cations in the sample will migrate most quickly because of EOF and their own mobility towards the cathode. Neutral particles introduced to the capillary will flow toward the cathode with the EOF, while anions migrate in the opposite direction. Because the EOF is usually higher than the

electrophoretic mobility of anions ($\mu_{eo} > \mu_{ep}$), the analyte anions can migrate toward the cathode with the cations but with lower velocity. Cations are the first to reach the detector as their observed (apparent, μ_{app}) mobilities are the sum of the electroosmotic mobility, μ_{eo}, of the solution and the electrophoretic mobility μ_{ep} (both have the same sign) Eq. 1.3:

$$\mu_{app} = \mu_{eo} + \mu_{ep} \tag{1.3}$$

Neutrals are detected the second they are moving with a velocity equal to EOF:

$$\mu_{app} = \mu_{eo} \tag{1.4}$$

Anions are the last to be detected because their apparent mobilities are the difference between μ_{ep} and μ_{eo} (different sign):

$$\mu_{app} = \mu_{eo} - \mu_{ep} \tag{1.5}$$

As the migration time for anions tends to be long, modification of electroosmotic flow and reversal of the polarity are helpful in attaining shorter analysis times. Modifying electroosmotic flow can be achieved by surface modification that imparts a positive charge on the wall of the capillary. This modification can be permanent or dynamic. The dynamic modification is usually accomplished with cationic surfactant. Velocity and the direction of EOF can be manipulated by using various types and concentrations of EOF modifiers. Alkyl ammonium salts are commonly used in most CE applications requiring the reduction or reversal of EOF.[38] Typically, modifiers are added to the separation buffer or are used to rinse the capillary before separation. Reversing the polarity (negative

polarity) then allows for the detection of anions where the anions move from the cathode (inlet) toward the anode (outlet), located at the detector end.

In addition to EOF modifiers and reversing the polarity, relative to chromatography, there are a large number of parameters that need to be considered when applying CE for separations including the composition of background electrolyte (BGE), pH, capillary dimensions, applied voltage and capillary temperatures.

1.4.2.3 Sample Injection

In capillary electrophoresis, a small volume of sample is injected into the capillary by hydrodynamic or electrokinetic injection. Hydrodynamic injection occurs by applying pressure at the inlet of the capillary (or vacuum at the exit end of the capillary). Injection time (several seconds) and pressure (several millibars) are the factors effecting sample injection volume. Hydrodynamic injection sample volume can be calculated using the Poiseulle equation:

$$V_i = \frac{\Delta p r^4 \pi t}{8\,\eta L} \tag{1.6}$$

where Δp is applied injection pressure, r *is* capillary radius, t is injection time, η is viscosity, and L is total length of the capillary. The length of the injected plug can be determined from the following equation:

$$Lp = \frac{V_i}{\pi r^2} = \frac{\Delta p r^2 t}{8\,\eta L} \tag{1.7}$$

In the absence of EOF and depending on the polarity, ions can also be injected. Electrokinetic injection is used to inject samples into a packed column capillary electrochromatography, as the samples cannot be pushed into a column containing

stationary phase with the low pressures that are used in hydrodynamic injection. Electrokinetic injection is performed by applying a voltage at both ends of the capillary for a period of time (seconds) to induce EOF which introduces analyte into the capillary. The sample injection quantity is directly related to the injection time, the magnitude of the voltage and the electrophoretic mobility.[48]

1.4.2.4 CE Separation Techniques for Inorganic Ions

The use of capillary electrophoresis has grown significantly more than other methods, such as IC, for analysis of inorganic anions in environmental and pharmaceutical samples as it offers several advantages such as rapid and efficient separation, minimal sample pretreatment, and low running cost. All CE modes are mainly derivatives or combinations of three basic types of electrophoresis: zone electrophoresis, isotachophoresis, and isoelectric focusing.[48] A CZE mode has been used for the separation of most sulfur anions with different detection techniques in a wide range of matrices.[50,51] Polarity of electrodes, applied voltage, temperature, capillary (internal diameter, and length), buffer (pH of a buffer), concentration/ionic strength of a buffer) and EOF modifier are the most important parameters that have been considered in CZE optimization. Modification of these parameters has allowed increased efficiency and fast electrophoretic separation to be achieved for sulfur-containing anions. As mentioned before, a reversal electrode polarization and EOF direction, or EOF reduction are required to detect analytes with a negative charge. Adding EOF modifiers and polarity switching affords fast separation of these analytes.[48] Changing buffer composition also helps to control the selectivity of separation by changing the mobility of the determined analytes.

1.4.2.5 Detection in Capillary Electrophoresis

A wide range of detectors can be used and are selected based on sensitivity, selectivity, dynamic range, and commercial availability. Some of the detection systems that have been employed with CE include UV-Vis absorption (direct and indirect modes), fluorescence, LIF (laser-induced fluorescence), and mass spectrometry, as well as conductivity, amperometric, radiometric, and refractive index (RI) detectors.[50] Table (1.1) shows the typical limit of detections (LODs) for various CE detection techniques. Some of them are more sensitive, which has led to lower LODs in CE (e.g., conductivity and mass spectrometry).

However, indirect and direct UV-Vis spectrophotometry are the most common detection techniques used in CE for sulfur analysis. The fused silica capillaries used in CE are transparent to UV and visible light allowing for a marriage with UV-Vis, making it the commercial instrument standard. With UV-Vis detection, ions with or without a chromophore are able to absorb light in the range of 190-900 nm.[48] CZE with indirect and direct UV-Vis spectrophotometry is less sensitive than other techniques that use the same detector, such as HPLC. This is partly due to small volume injection in CE compared with that for HPLC. UV-Vis detection occurs by measuring transmitted light. It means the optical path is equal to the internal diameter of the cell. CZE-UV-Vis detection is also less sensitive due to its short path length dictated by the diameter of the fused silica capillary. Extending the light path improves the sensitivity of CZE-UV-Vis detection at a low injection volume such as a ‘‘bubble cell’’ capillary, and a Z-shaped cell.[48]

Table 1.1. Detection methods in CE and detection limits.[48]

Detection Mode	Typical LOD range (M)
Direct UV absorption	$10^{-5} – 10^{-7}$ (standard pathlength)
	10^{-8} (extended pathlength)
Indirect UV absorption	$10^{-5} – 10^{-7}$
Direct laser-induced fluorescence LIF (on-column)	$10^{-10} – 10^{-11}$
Direct on- column LIF	10^{-16}
Post-column LIF	10^{-16} (single molecule)
Refractive index	$10^{-5} – 10^{-6}$ (capillary)
	10^{-5} (microchip)
Conductivity	$10^{-7} – 10^{-9}$
Amperometry	$10^{-7} – 10^{-10}$
Potentiometry	$10^{-7} – 10^{-8}$
Raman	$10^{-3} – 10^{-6}$ (pre-concentration required)
MS	$10^{-8} – 10^{-10}$

1.4.2.5.1 CE with Direct Spectrophotometric Detection

Direct UV-Vis detection in CE is sensitive for analytes with high UV absorbance, such as thiosulfate and polythionates. The electrolyte that is used in direct UV-Vis detection should have very low or no absorption at the desired measurement wavelength to ensure the highest detection sensitivity.[38,48] Absorbance in direct UV-Vis appears as positive peaks proportional to analyte concentration and absorptivity. A strongly absorbing background electrolyte will can lead to a noisy baseline, which is more problematic if the analyte absorptivity is low. Electrolyte pH has a significant effect on analyte mobility, which in turn affects the selectivity. To achieve high resolution, the BGE must have ions with electrophoretic mobility closely matched to that of the ions of interest. LOD for direct UV-Vis detection is generally in the range of 10^{-5}–10^{-6} M which can be decreased by extending the capillary pathlength.[48] However, some inorganic anions are completely transparent to UV-Vis or only weakly absorbing. In such cases, the ions cannot be detected or sensitivity is poor, which necessitates indirect detection.

1.4.2.5.2 CE with Indirect Spectrophotometric Detection

CE with indirect detection is a universal technique designed for detection of those analytes that do not show absorption of UV-Vis light including sulfate and sulfite. For indirect detection, a highly absorbing chromophore is added to the carrier electrolyte to create a high absorbance background signal. Non-absorbing ions are separated into zones as a function of their electrophoretic mobilities. In these zones, the non-absorbing ions displace chromophore ions as a result of charge repulsion as both have the same charge. When the zone of non-absorbing analyte reaches the detector, the decrease of absorbance

is observed (negative peak). The negative peaks produced can be inverted to produce a "normal" electropherogram by using a reference wavelength. The following background chromophore ions are commonly used for detection of non-absorbing anions including chromate, pyromellitic acid, phthalates, and naphthalenesulfonic acid while 1-naphthylamine, quinine, or malachite green are used for cations.[48] The background chromophore ions must be compatible with the analysis conditions and feature similar mobility to the mobility of the analyte, have high molar absorption coefficient at chosen detection wavelength which provides large absorbance drop after the chromophore ions are displaced by the sample ions, and be unreactive toward the analytes. The concentration of the chromophore probe affects the peaks shape. The optimal concentration should be a compromise between high linearity range and low noise level, and achieving symmetrical peak shape.

1.5 Research Objectives and Organization of Thesis

The development of fast and sensitive methods using CE with direct and indirect methods was the primary objective of this research. These methods were employed for the analysis of different sulfur species such as, sulfide (S^{2-}, HS^-), sulfate (SO_4^{2}), sulfite (SO_3^{2-}), and thiosalts ($S_xO_y^{2}$) in produced water and reservoir water. Another requirement in analysis of sulfur-containing anions was to assess their stability under different conditions (e.g., temperature, pH) that represent in situ and laboratory conditions. Detecting and quantifying these species in the oil and gas reservoirs will provide information that will lead to a better understanding of hydrogen sulfide and thiosalts chemistry, which is needed to develop the best treatment protocols. During CZE with direct and indirect UV

detection, several parameters affecting the selectivity and sensitivity such as electroosmotic flow modifiers, selection of chromophoric probes, pH, and cassette temperature were optimized. The introduction of hydrogen sulfide and thiosalt generation, as well as an overview of the analytical approaches for their analysis is presented in this chapter. Chapter 2 is a report of studies of the influence of several method parameters, such as the type and concentration of BGE chromophoric probe and EOF modifiers, pH and separation temperature. The method was also applied to the analysis of real samples in Chapter 2. Chapters 3 and 4 focus on the challenges presented during the development of an indirect CZE method for sulfur species analysis; Chapter 3 describes the reactivity of sulfite and tetrathionate and the effect of sulfide; Chapter 4 illustrates oxidation-reduction reactions for sulfur-oxygen species during sulfur species analysis with CZE-UV-Vis method.

1.6 Co-Authorship Statement

All research and experiments were carried out by Saeed, with input and advice from Dr. Christina Bottaro and Dr. Ali Modir-Rousta. The entire manuscript was prepared by Saeed with advice and editing assistance provided by Dr. Bottaro.

1.7 References

(1) Al-Zahrani, I.; Basheer, C.; Htun, T. *J. Chromatogr. A* **2014**, *1330*, 97–102.

(2) Okoro, C.; Smith, S.; Chiejina, L.; Lumactud, R.; An, D.; Park, H. S.; Voordouw, J.; Lomans, B. P.; Voordouw, G. *J. Ind. Microbiol. Biotechnol.* **2014**, *41* (4), 665–678.

(3) Hißner, F.; Mattusch, J.; Heinig, K. *Fresenius. J. Anal. Chem.* **1999**, *365* (8), 647–653.

(4) El-hady, D. A. **2009**, *64* (11), 1166–1173.

(5) Schippers, A., & Sand, W. *Applied and Environmental Microbiology*. **1999**, *65*(1), 319–321.

(6) Clark, P. D.; Hyne, J. B.; David Tyrer, J. *Fuel* **1984**, *63* (1), 125–128.

(7) Druschel, G. K.; Baker, B. J.; Gihring, T. M.; Banfield, J. F. *Geochem. Trans.* **2004**, *5* (2), 13–32.

(8) Gieg, L. M.; Jack, T. R.; Foght, J. M. *Appl. Microbiol. Biotechnol.* **2011**, *92* (2), 263–282.

(9) Mougin, P.; Lamoureux-Var, V.; Bariteau, A.; Huc, A. Y. *J. Pet. Sci. Eng.* **2007**, *58* (3–4), 413–427.

(10) Machel, H. . *Sediment. Geol.* **2001**, *140* (1–2), 143–175.

(11) Holubnyak, Y.; Bremer, J. M.; Hamling, J. A.; Huffman, B. L.; Mibeck, B.; Klapperich, R. J.; Smith, S. A.; Sorensen, J. A.; Harju, J. A. In *SPE International Symposium on Oilfield Chemistry*; Society of Petroleum Engineers, **2011**, 2, 889-896.

(12) Guenther, E. A.; Johnson, K. S.; Coale, K. H. *Anal. Chem.* **2001**, *73* (14), 3481–

3487.

(13) Marcano, N. *Geoscience engineering*, **2013**, 35(3), 2–5.

(14) Pavlova, A.; Ivanova, P.; Dimova, T. *Pet. Coal*, **2012**, *54* (511), 9–13.

(15) Truong, D. H.; Eghbal, M. a; Hindmarsh, W.; Roth, S. H.; O'Brien, P. J. *Drug Metab. Rev.* **2006**, *38* (4), 733–744.

(16) Jiang, J.; Chan, A.; Ali, S.; Saha, A.; Haushalter, K. J.; Lam, W.-L. M.; Glasheen, M.; Parker, J.; Brenner, M.; Mahon, S. B.; Patel, H. H.; Ambasudhan, R.; Lipton, S. A.; Pilz, R. B.; Boss, G. R. *Sci. Rep.* **2016**, *6* (October 2015), 20831.

(17) Kellogg, W. W.; Cadle, R. D.; Allen, E. R.; Lazrus, A. L.; Martell, E. A. **1972**, *175* (4022), 587–596.

(18) Luther, G. W. I.; Giblin, A. E.; Varsolona, R. *Limnol. Oceanogr.* **1985**, *30* (4), 727–736.

(19) Druschel, G. K.; Hamers, R. J.; Banfield, J. F. *Geochim. Cosmochim. Acta* **2003**, *67* (23), 4457–4469.

(20) Xu, Y.; Schoonen, M. A. A.; Nordstrom, D. K.; Cunningham, K. M.; Ball, J. W. *J. Volcanol. Geotherm. Res.* **2000**, *97* (1–4), 407–423.

(21) Kuijvenhoven, C.; Bostock, a.; Chappel, D. *SPE Int.* **2005**, No. SPE 92795, 9.

(22) Tang, K.; Baskaran, V.; Nemati, M. *Biochem. Eng. J.* **2009**, *44* (1), 73–94.

(23) da Silva, M. L. B.; Soares, H. M.; Furigo, A.; Schmidell, W.; Corseuil, H. X. *Appl. Biochem. Biotechnol.* **2014**, *174* (5), 1810–1821.

(24) Krouse, H. R.; Viau, C. A.; Eliuk, L. S.; Ueda, A.; Halas, S. *Nature* **1988**, *333*, 415–419.

(25) Ma, Q.; Ellis, G. S.; Amrani, A.; Zhang, T.; Tang, Y. *Geochim. Cosmochim. Acta*

2008, *72* (18), 4565–4576.

(26) Wang, G. L.; Li, N. X.; Gao, B.; Li, X. Q.; Shi, S. B.; Wang, T. G. *Chinese Sci. Bull.* **2013**, *58* (28–29), 3588–3594.

(27) Chen, T.; He, Q.; Lu, H.; Peng, P.; Liu, J. *Sci. China, Ser. D Earth Sci.* **2009**, *52* (10), 1550–1558.

(28) Cai, C.; Worden, R. H.; Bottrell, S. H.; Wang, L.; Yang, C. *Chem. Geol.* **2003**, *202* (1–2), 39–57.

(29) Moses, C. O.; Kirk Nordstrom, D.; Herman, J. S.; Mills, A. L. *Geochim. Cosmochim. Acta* **1987**, *51* (6), 1561–1571.

(30) Peters, E. *Metall. Trans. B* **1976**, *7* (4), 505–517.

(31) Marsland, S. D.; Dawe, R. a; Kelsall, G. H. *SPE Int. Symp. Oilf. Chem.* **1989**, 201–206.

(32) Arsanova, G. I. *J. Volcanol. Seismol.* **2014**, *8* (6), 361–374.

(33) Kuyucak, N.; Yaschyshyn, D. *Environment IV Conference*, **2007**, 3(705). 45-51.

(34) Fahd, F.; Khan, F.; Hawboldt, K.; Abbassi, R. *Stoch. Environ. Res. Risk Assess.* **2013**, *28* (2), 383–391.

(35) Druschel, G. K.; Schoonen, M. A. A.; Nordstrom, D. K.; Ball, J. W.; Xu, Y.; Cohn, C. a. *Geochem. Trans.* **2003**, *4* (3), 12.

(36) Chen, Z.; Naidu, R. *Int. J. Environ. Anal. Chem.* **2003**, *83* (9), 749–759.

(37) O'Reilly, J. W.; Dicinoski, G. W.; Shaw, M. J.; Haddad, P. R. *Anal. Chim. Acta* **2001**, *432* (2), 165–192.

(38) Padarauskas, A.; Paliulionyte, V.; Ragauskas, R.; Dikcius, A. *J. Chromatogr. A* **2000**, *879* (2), 235–243.

(39) Divjak, B.; Goessler, W. *J. Chromatogr. A* **1999**, *844* (1–2), 161–169.

(40) Haddad, P. R.; Doble, P.; Macka, M. *Journal of chromatography* **1999**, *856* (99), 145–177.

(41) Haddad, P. R. *J. Chromatogr. A* **1997**, *770* (1–2), 281–290.

(42) Chen, M. L.; Ye, M. L.; Zeng, X. L.; Fan, Y. C.; Yan, Z. *Chinese Chem. Lett.* **2009**, *20* (10), 1241–1244.

(43) Motellier, S.; Descostes, M. *J. Chromatogr. A* **2001**, *907* (1–2), 329–335.

(44) Safizadeh, F.; Larachi, F. *Instrum. Sci. Technol.* **2014**, *42* (3), 215–229.

(45) Hissner, F.; Mattusch, J.; Heinig, K. *J. Chromatogr. A* **1999**, *848* (1–2), 503–513.

(46) Wiederschain, G. Y. *Handbook of capillary and microchip electrophoresis and associated microtechniques (3rd Edn.)* **2008**, 73.

(47) Tiselius, A. *Trans. Faraday Soc.* **1937**, *33*, 524–531.

(48) Buszewski, B.; Dziubakiewicz, E.; Szumski, M. *Electromigration Techniques* **2013**, 105.

(49) Lu, Y.; Gao, Q.; Xu, L.; Zhao, Y.; Epstein, I. R. *Inorg. Chem.* **2010**, *49* (13), 6026–6034.

(50) De Carvalho, L. M.; Schwedt, G. *J. Chromatogr. A* **2005**, *1099* (1–2), 185–190.

(51) Petre, C. F.; Larachi, F. *J. Sep. Sci.* **2006**, *29*, 144–152.

Chapter 2. Indirect and Direct Capillary Electrophoresis: Method Development for the Determination of Sulfide Anions and Sulfur Oxyanions in Oil Reservoir Fluids

2.1 Introduction

Sulfides and sulfur oxyanions (e.g., thiosulfate, sulfate, polythionates, etc.) play an important roles in the environment, in a number of industrial processes, as well as in the metabolism of organisms. In particular, some of these compounds can impact environmental quality, exhibit toxicity, and can have negative economic consequences.[1] They are related by various oxidation and reduction reactions which are generated in a sulfur cycle.[2-6] Sulfur-oxygen species entering the environment due to industrial activities can be reduced to corrosive and toxic forms such as sulfide in anaerobic environments.[6,7] Partially oxidized forms of sulfur are undesirable as they can acidify the environment upon oxidation, and mobilize toxic metals. Perhaps the most negative impact of the sulfur cycle in terms of offshore oil and gas operations is the increase cost of production due to the cost of treatment or refit of damaged equipment.[2-4] Comprehensive data about sulfur speciation in environmental samples is essential to better understand many environmental processes and to monitor reduction or oxidation reactions in offshore oil and gas operation. Analysis of sulfur-containing ions has traditionally been difficult as the mixture can be very complex, often accompanied by other anions, inorganic and organic compounds, and typically occur at low concentrations.[1,5] The chemistry of such solutions is quite complicated since certain species react with each other, decompose or become oxidized by air. Sometimes the analytical technique used and sample storage can cause changes in the composition of the samples.[2,8,9] Therefore, fast analytical methods that

give specific and sensitive determination of the substances of interest are required. IC and CZE with various detection techniques have been applied to determine sulfur-containing anions. Separation techniques are chosen for their selectivity, low limit of detection, and good tolerance to sample matrices. CZE is used as an attractive method of separation and as an alternative to IC because it is more efficient, faster, more operational, and more economical. CZE methods can also conduct the analysis in a complex matrix such as saline water and identify all of the ions of interest. Though CZE methods are typically less sensitive (e.g., low sample volume injection and small capillary diameter), they are efficiently wrapped due to coupling with direct and indirect UV-Vis detection.[1,5,10,11,12,13]

CZE is frequently coupled with UV-Vis with either indirect or direct detection to provide fast electrophoretic separation for sulfur species. Direct UV detection allows for the detection of absorbing anions such as thiosulfate, sulfide, and polythionate, while indirect UV detection is used for the detection of non-absorbing species or for anions that show little direct UV absorbance such as sulfate. To provide fast separation, to achieve optimal peak shape and sensitivity, a strategy that combines CZE methods with both direct and indirect detection has been expanded for the detection and quantification of charged sulfur species; SO_4^{2-}, $S_2O_3^{2-}$, $S_4O_6^{2-}$, SO_3^{2-}, and HS^- in high salinity of real samples (e.g., produced water) that were obtained from an offshore oil and gas operator.[1,3,14] The components of the background electrolyte (e.g., pH (buffers), flow modifiers, chromophoric probes, etc.) have been studied and optimized for each method. For example, indirect detection requires a chromophoric probe to enhance detection sensitivity for some sulfur-containing species.[1] The most common chromophoric probes for the analysis of sulfur oxyanion species in CZE are chromate (CrO_3^{2-}) and

pyromellitate, where they are both in the fully ionized form of chromic acid solution (H_2CrO_4) and pyromellitic acid (PMA, benzene-1,2,4,5- tetracarboxylic acid (Figure 2.1)), respectively. Probes such as chromate (CrO_3^{2-}) can interact negatively as an oxidizing agent for some sulfur species. As demonstrated during the method optimization process (Section 2.3.2), pyromellitate is non-oxidizing, has high molar absorptivity (high sensitivity), and is an ideal mobility match for thiosalts, which reduces dispersion. Electrophoretic mobility of the background ion and sulfur species should be the same to achieve optimal peak shape and sensitivity. However, the existing methods do not work for saline water and have not been applied to analytes of interest in this work, specifically thiosulfate and chloride.[1] This problem was solved by applying a direct method of analysis as this method involves less interference from non-absorbing species present in saline water. The CZE methods were developed in negative polarity, which usually leads to long migration times because the anions migrate towards the detector, and oppose EOF. HMOH is added as an EOF modifier to influence the chemistry of the capillary surface, yielding shorter times of analysis and characteristics. pH systems have been used to change migration time by modifying the charge of the analytes, to maximize the resolution between co-migrating ions, and to control the ionization of PMA.[1,12,15,16]

Other required features of the method that affect separation time and efficiency include capillary length, separation temperature, applied potential, and use of a stabilizing agent to limit spontaneous oxidation of some of sulfur-containing compounds.

2.2 Materials and Methods

2.2.1 Materials

All chemicals used for this work were of analytical grade and obtained from Sigma-Aldrich unless otherwise noted. Chromic acid (H_2CrO_4), was prepared by dissolving chromium trioxide CrO_3 in water, and PMA were investigated as a chromophoric probe in indirect CZE. Since EOF increases with pH values greater than 3, an EOF modifier, hexamethanium hydroxide (HMOH 0.1 M) was introduced to the running buffer solution to reduce the surface charge on the capillary and suppress EOF. BIS [2-hydroxyethylaminotris[hydroxymethyl]methane (BIS-TRIS >98% purity) at pH 7.0, triethanolamine (TEA) at pH 8.0, ammonium hydroxide (NH_4OH >99% purity) at pH 9.0 were used for pH control in the various BGE systems. Formic acid (CH_2O_2 pK_a=3.75) was used to adjust pH to 9.0 in the BGE containing HMOH and NH_4OH in the direct detection method. Diethylenetriaminepentacetic acid (DTPA > 99% purity) was used as a stabilizing agent for sulfur oxyanion species (Figure 2.2). CE grade sodium hydroxide solution (1.0 M) was purchased from Agilent Technologies Canada Inc., Mississauga, ON. All water used for this work was optima LC/MS water (suitable for UHPLC-UV, Fisher Chemical, UK). Stock solutions of 1000 mg/L of sulfur oxyanion salts dissolved in nitrogen- bubbled deoxygenated LC water containing DTPA 0.1 mM were prepared from sodium sulfate anhydrous ($Na_2SO_4 \geq 90.0\%$), sodium thiosulfate ($Na_2S_2O_3 \geq 99.9\%$ purity), potassium tetrathionate ($K_2S_4O_6$ > 99.9% purity), sodium sulfite anhydrous ($Na_2SO_3 \geq 90.0\%$), sodium sulfide (Na_2S), sodium hydrosulfide hydrate (HNaS. xH2O) and sodium chloride (NaCl ≥ 99.0). These solutions were kept in amber bottles at 4°C,

except when being analyzed.[3,17] Working solutions were prepared fresh daily. Deoxygenation solutions with nitrogen and addition of DTPA were key to the preparation of stable solutions of sulfur-oxyanions, as these anions are easily oxidized in the presence of oxygen and other impurities such as iron(III) or copper(II).[3,17,18] DTPA increases sulfur species stability by chelating trace metals, which otherwise catalyze the oxidation in air.[17] At low concentrations (0.1 mM), DTPA does not interfere with spectrophotometry.[19] All solutions were degassed and filtered with a 0.22 µm nylon syringe filter (Canadian Life Science, ON).

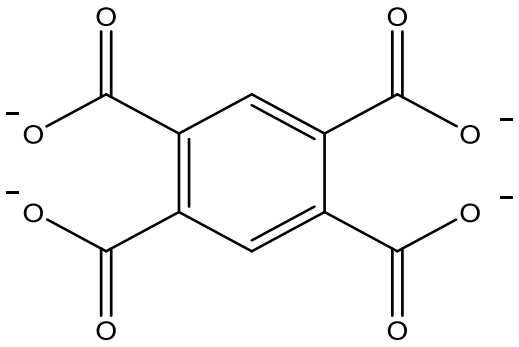

Figure 2.1. Ionized form of pyromellitic acid (PMA).

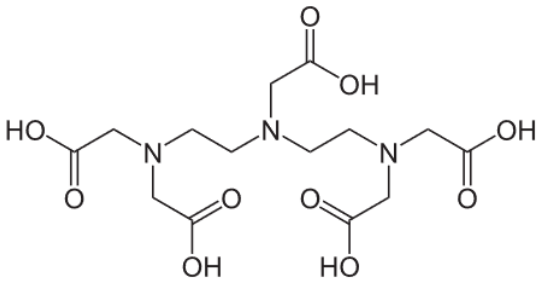

Figure 2.2. Diethylenetriaminepentaacetic acid (DTPA).

2.2.2 Instrumentation

All experiments were performed with an Agilent 7100 ^{3D}CE System (Agilent Technologies Canada Inc., Mississauga, ON) equipped with a UV-Vis diode array detector (DAD). The system DAD allows for monitoring at different wavelengths (200, 230, 214, and 254 nm) which provides for selection of wavelengths that give the highest sensitivity. The reason for selecting these wavelengths was to gain more information about sulfur anion species. Signals were monitored at 360 nm with a reference of wavelength of 214 nm for indirect detection (using λ_{max} for the reference wavelength will invert the negative peaks), while signals at 214 nm with 360 nm as the reference wavelength were collected for direct detection. Standard bare fused-silica capillaries (50 μm i.d. (internal diameter) and 360 μm o.d. (outer diameter)) were obtained from MicroSolv Technology Corporation (NJ, USA), and cut to total lengths of 64.5 cm (56 cm to the detector), and 48.5 cm (40 cm). A MicroSolv Window Maker™ (N.J. USA) was used to burn the external polyimide coating from the capillaries at 8.5 cm to create a detection window and also at the last 2 mm of the ends. The potential was ramped over 1 min from zero to a constant -30 kV for the separation. Corrected peak areas, peak widths and heights, and migration times were determined using Agilent OpenLAB Chromatography Data System (CDS) ChemStation.

Initial capillary conditioning was as follows: flushing at ~ 940 mbar with methanol for 10 min, water for 5 min, 1.0 N NaOH for 20 min, water for 20 min and BGE for another 30 min. Daily capillary conditioning was with 0.1 N NaOH for 3 min, water for 3 min and BGE for another 6 min. Between consecutive runs, the capillary was flushed with 0.1 N NaOH for 1 min, water for 1 min and BGE for 3 min. Samples were

injected hydrodynamically by an overpressure of 20 mbar for 5 s from the inlet vial (cathodic end). The temperature of the capillary loading was maintained at 25 °C for all experiments. A Varian Cary 6000i UV-Vis-NIR spectrophotometer (Agilent Technologies Canada Inc., Mississauga, ON) with 1 cm quartz cuvettes (International Crystal Laboratories, NJ, USA) was used for UV-Vis analysis to determine λ_{max} and molar extinction coefficients of the sulfide, thiosalt species and the chromophoric probe.

2.3 Results and Discussions

The method parameters (chromophoric probe, pH, EOF modifier, capillary length and temperature) were optimized in a univariate approach (one factor at a time) with ranges chosen according to methods reported in the literature, along with previous experiments on thiosalt standards done by Pappoe et al. (2014).[1,5,10-13,20] Optimum concentrations might be determined be values either lower or higher levels than reported in the literature; hence they are included to avoid unwarranted constraints.

2.3.1 UV-Vis Analysis of Sulfide and Thiosalts Species

UV-Vis analysis of the sulfide, thiosalt species and PMA was used to determine their molar absorptivities at the absorbance maxima (λ_{max}). Ideally, with indirect detection, a wavelength is chosen at, or close to, the absorption maximum of the chromophoric probe to obtain the largest signal and in which the analyte does not absorb. The maximum absorption of PMA is 214 nm, as shown in (Figure 2.3). The maximum absorption is 230 nm for S^{2-} and HS^-, 214 nm for $S_2O_3^{2-}$ and $S_4O_6^{2-}$, while there is no absorption for SO_4^{2-}, SO_3^{2-}, and Cl^- (Figure 2.4). Different wavelengths have been used (200, 230, 214, and 254 nm) to achieve the highest sensitivity since CE is equipped with DAD. The most

sensitive results for non-absorbing species showed at 214 nm in the indirect method. To invert the negative peaks and register them as positive peaks, absorbance was measured at 360 nm with the reference wavelength at 214 nm. When non-absorbing ions displace the PMA, the decrease in absorbance at 214 nm will be greater than that at 360 nm. Absorbing sulfur species such as S^{2-}, HS^{-}, $S_2O_3^{2-}$ and $S_4O_6^{2-}$ decrease the sensitivity for the indirect mode, hence direct detection is possible.

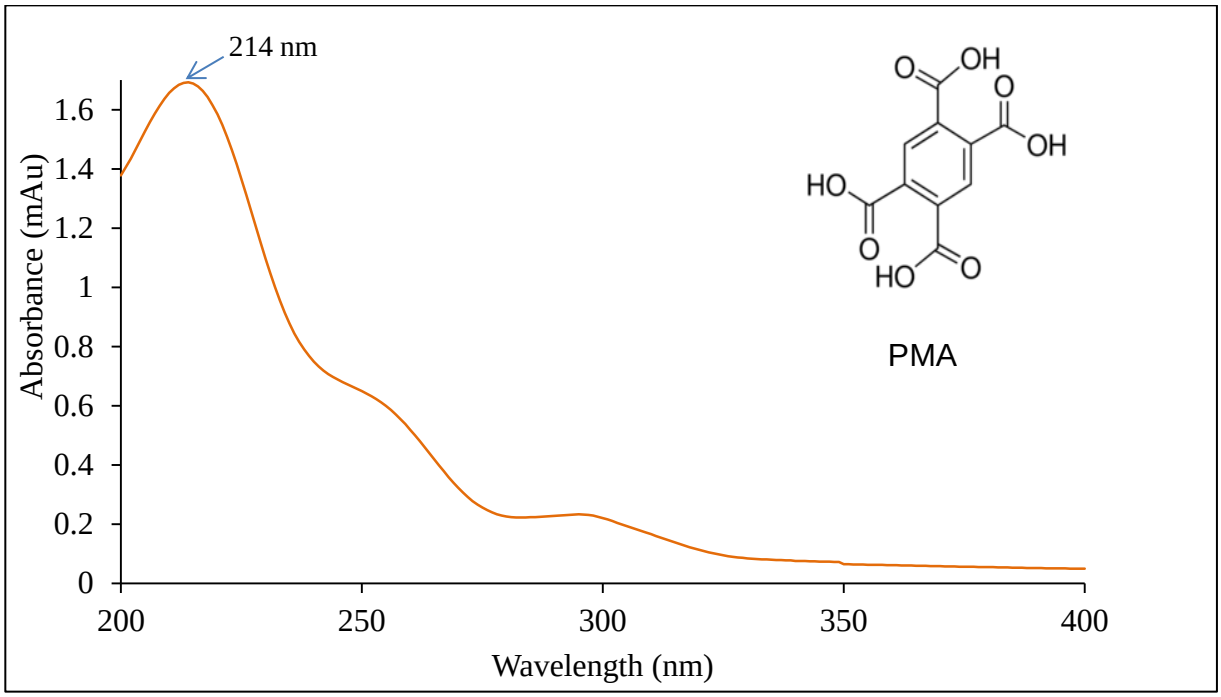

Figure 2.3. UV-Vis absorption spectra of PMA (0.06 mM).

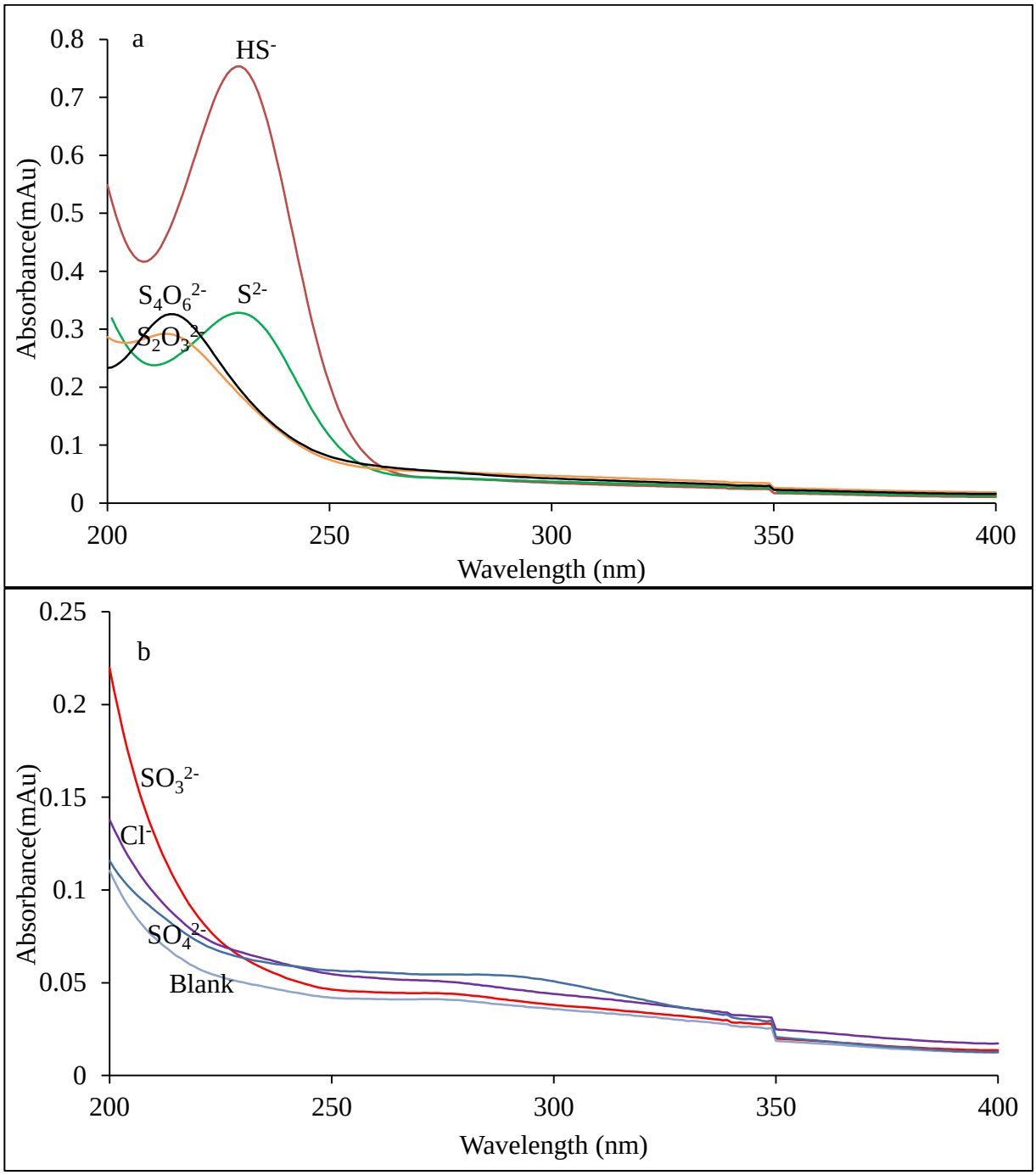

Figure 2.4. UV-Vis spectra of a) absorbing anions HS^- (0.143 mM), S^{2-} (0.103 mM), $S_2O_3^{2-}$ (0.064 mM), $S_4O_6^{2-}$ (0.026 mM), b) non-absorbing anions SO_3^{2-} (0.063 mM), SO_4^{2-} (0.056 mM), all anions in DTPA solution 0.1 mM.

2.3.2 Influence of PMA

The presence of a chromophoric probe in the separation buffer in indirect CZE provides a background signal and improves detection sensitivity for anions that do not absorb enough for CE with direct detection. During electrophoretic separation in the CZE, the analyte ions form zones (termed eigenzones) as a function of their electrophoretic mobilities. In eigenzones, the composition of the BGE is slightly different from the surrounding buffer environment because of the charge repulsion between analytes of the same charge, which causes displacement of the chromophoric probe ions and reduces their concentration in the analyte zone. This competitive process leads to a reduction in the background absorption that results in negative peaks. The peak area is proportional to the molar concentration of the analytes in the eigenzone. For a high-resolution separation to occur, an electrolyte optimal for common inorganic anions must have a chromophore with electrophoretic mobility closely matched to that of the anions of interest. Chromate anions (CrO_3^{2-}) and pyromellitate anions are the most common chromophoric probes for the analysis of sulfur oxyanion species in CZE as both are the conjugate base of chromic acid solution (H_2CrO_4) and PMA, respectively. Both probes were titrated with TEA to pH 8.0. Chromate has some limitations as it is an oxidizing agent which makes it unsuitable for use with some sulfur-oxygen species.[9,21]

In Figure 2.5 (a, b), 2.0 mM of PMA and CrO_3^{2-} probes were tested on a mixture of non-absorbing SO_4^{2-} and SO_3^{2-} in which the pH was adjusted to 8.0 using TEA. In both probes, a system peak appeared. With PMA, SO_4^{2-} was identified, while SO_3^{2-} was oxidized to SO_4^{2-} due the fact that SO_3^{2-} is oxidized in the presence of oxygen and metal impurities (Section 3.5.1).[14] With chromate, both SO_3^{2-} and SO_4^{2-} completely disappeared

and precipitation was observed, causing deterioration of the baseline. Although the nature of the precipitation was not identified, its presence provides evidence that chromate catalyzed the reaction causing a decline of the slope and loss of the analyte. However, PMA is non-oxidizing, has high molar absorptivity, and demonstrates a close mobility match with the sulfur oxyanions, which results in good peak characteristics because of reduced electromigration dispersion. Hence, PMA was chosen for this work.[1,22]

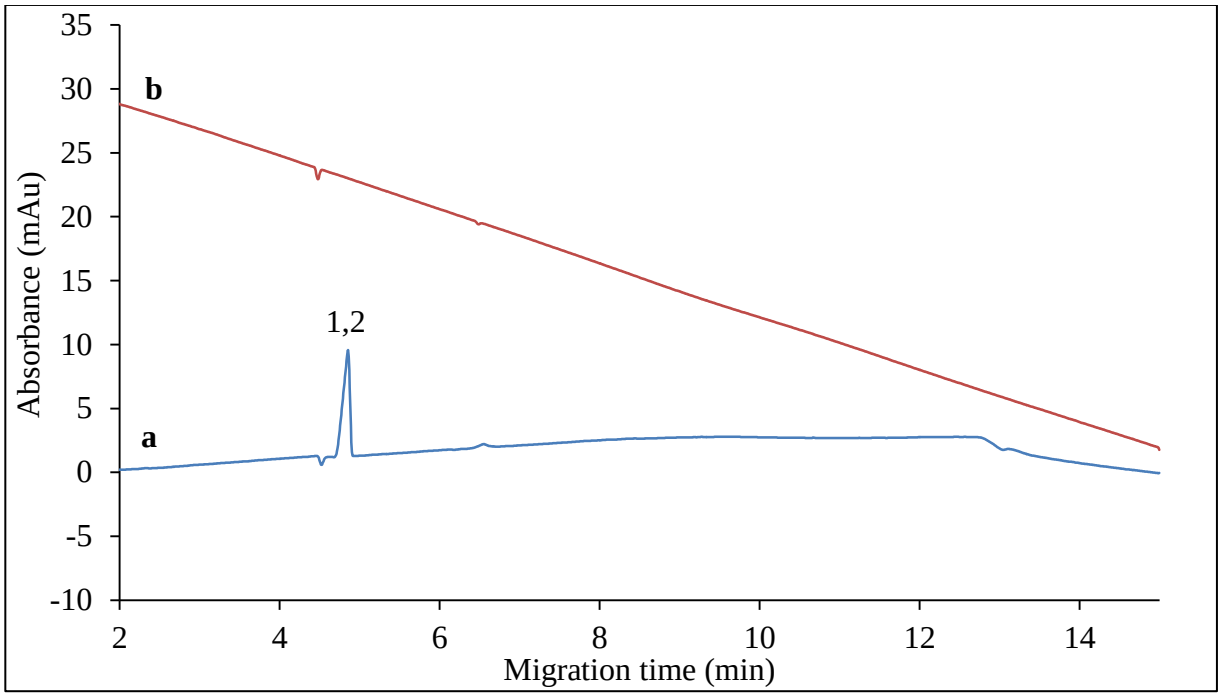

Figure 2.5. Mixture of 1) SO_4^{2-} 0.70 mM, 2) SO_3^{2-} 0.79 mM, BGE: a) PMA 2.0 mM, b) CrO_3^{2-} 2.0 mM, HMOH 0.8 mM, adjusted to pH 8.0 with TEA, CE conditions: capillary length 64.5 cm, injection 50 mbar for 5 s, applied voltage -30 kV at 25 °C. Spectra acquired at wavelength 360 nm with reference at 214 nm.

The concentration of the PMA can impact selectivity and sensitivity. Therefore, a range of PMA concentrations were studied to determine which concentration would be

ideal for the analysis. Pappoe et al. (2014) reported the use of PMA at 2.00 mM. The range in this project was expanded and studied at five concentrations ranging from 2.00 mM to 8.0 mM to ensure that optimal signal intensity was obtained.[1,20] These ranges were prepared by mixing PMA with HMOH in different ratios (1:4, 1:2, 1:1, 2:1, 5:1). The solution injections were 20 mbar for 5 seconds followed by injected water at 50 mbar for 10 seconds with an auxiliary applied pressure of 50 mbar. As would be expected with increasing the concentration of PMA, the absorptivity of the BGE increased as shown in Figure. 2.6. From these results, it can be concluded that a linear response with respect to the concentration is stable up to about 7.0 mM and the molar displacement of the chromophoric probe by analyte ions should be linear. Increasing PMA concentration causes increased ionic strength which negatively impacts migration time; hence 6.0 mM of PMA was chosen as the optimum value.

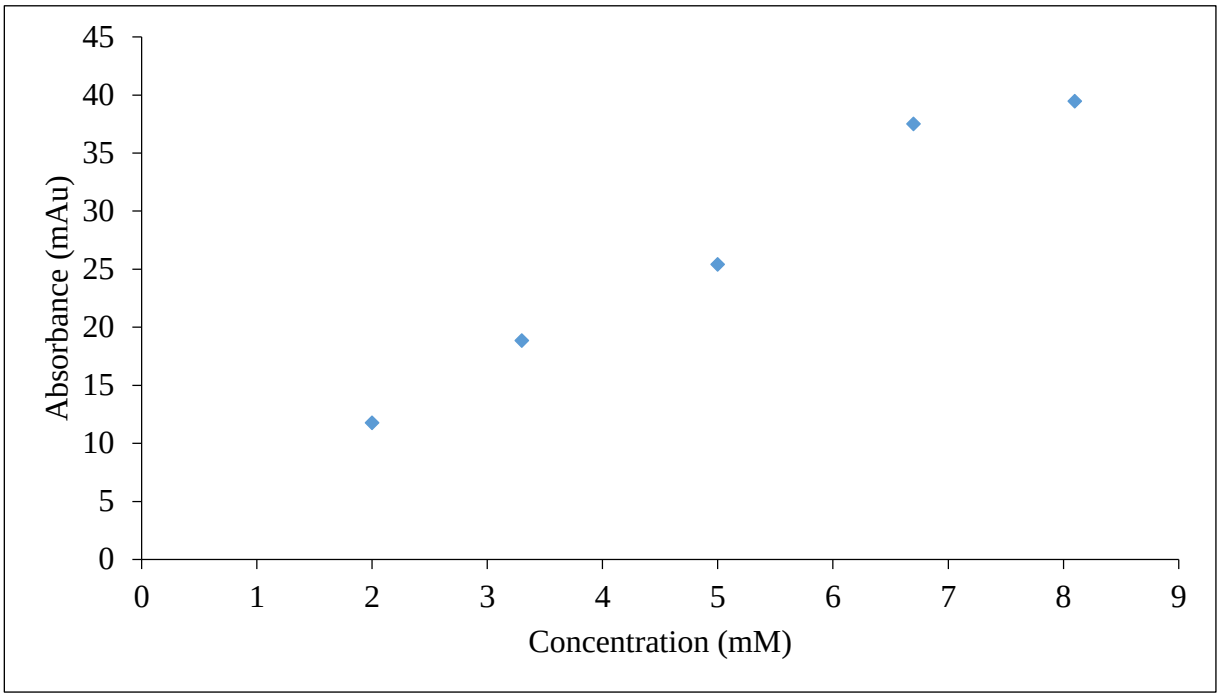

Figure 2.6. PMA 2.0, 3.0, 5.0, 6.0, 8.0 mM. Capillary length 64.5 cm, injection 20 mbar for 5 s. Auxiliary applied pressure 50 mbar, temperature 25°C.

2.3.3 Influence of pH

The pH can have a significant effect on solute mobility, and therefore it can manipulate the separation selectivity.[1] Specifically, the pH impacts migration time and maximizes the resolution between co-migrating ions by modifying the charges which occur at or near pK_a for the analyte. It also controls the ionization of HMOH and PMA to obtain optimal peak shape and sensitivity. Furthermore, electrolyte pH impacts the EOF by affecting the ionic strength (conductivity) of the electrolyte.[1] The pH must be carefully controlled as pH fluctuations cause problems with selectivity and reproducibility of migration time and peak area. Weakly basic conditions are favoured (pH 7-9) since thiosulfate is decomposed in acidic media.[1,3] At these pHs, the effective mobility of weak ionic sulfur species

(sulfite and sulfide) is also significantly increased since the pH is above the analyte pK_as (HSO_3^-/SO_3^{2-} 1.89, 7.21, HS^-/S^{2-} 6.9, 12.9), and leads to the ionization of solutes.[1,9,23,24] Furthermore, complete ionization for PMA occurs at pH >6 (pK_{a1}= 1.92, pK_{a2}= 2.87, pK_{a3}= 4.49, pK_{a4}= 5.63) which provides a stable absorbance profile and reproducible migration behaviour. For these reasons, the performance of three different bases including bis[2 -hydroxyethyl]aminotris[hydroxymethyl]-methane (BIS-TRIS, pK_a= 6.5) pH 7.0 (Figure. 2.7), triethanolamine (TEA, pK_a= 7.74) pH 8.0 (Figure 2.8), and ammonium hydroxide (NH_4OH, pK_a= 9.25) pH 9.0 were studied. For the BGE, the probe was titrated to pH 7.0 with BIS-TRIS, to pH 8.0 with triethanolamine, and to pH 9.0 with ammonium hydroxide to form buffered background electrolyte solutions containing 2.0 mM PMA and 0.8 mM HMOH. Figure 2.9 shows that better separation and optimal peak symmetry for the separation of the $S_2O_3^{2-}$, Cl^-, SO_4^{2-}, $S_4O_6^{2-}$, and SO_3^{2-} mixture was obtained by using the ammonium buffered background electrolyte. However, there was co-migration between $S_4O_6^{2-}$, and SO_3^{2-}.

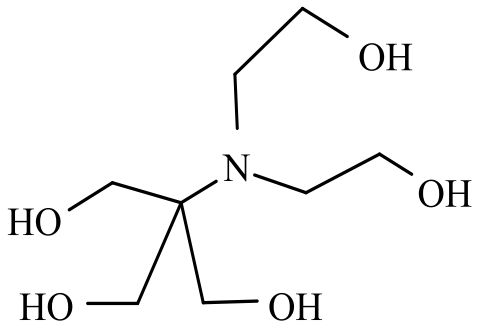

Figure 2.7. Bis[2 -hydroxyethyl] aminotris[hydroxymethyl]-methane (BIS-TRIS).

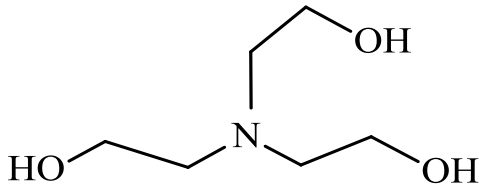

Figure. 2.8. Triethanolamine (TEA).

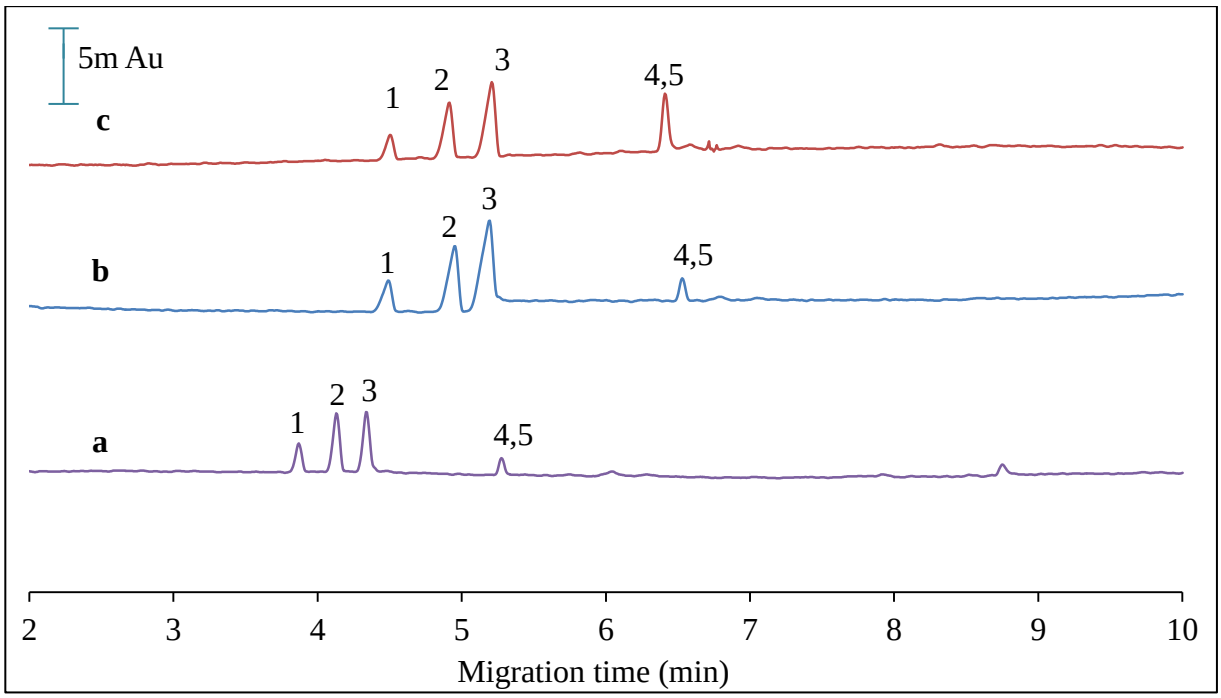

Figure 2.9. Sample: mixture of 1) $S_2O_3^{2-}$ 0.20 mM, 2) Cl^- 0.86 mM, 3) SO_4^{2-} 0.35 mM, 4) $S_4O_6^{2-}$ 0.17 mM, 5) SO_3^{2-} 0.40 mM. BGE: PMA 2.0 mM, HMOH 0.8 mM, DTPA 0.1 mM plus pH adjusted to a) pH 7.0 with BIS-TRIS, b) pH 8.0 with TEA, c) pH 9.0 with NH_4OH. CE conditions: capillary length 64.5 cm, injection volume 20 mbar for 5 s, applied voltage -30 kV at 25 °C. Spectra acquired at 360 nm with reference at 214 nm.

The concentrations of NH_4OH were further optimized after PMA and HMOH optimization as was explained in Sections 2.3.2, and 2.3.4. The optimized buffer system was determined to be 6.0 mM PMA and 1.0 mM HMOH, with pH adjusted to 9.0 with NH_4OH by titration. The concentrations of NH_4OH were varied to test their effects on the separation. First, NH_4OH with a concentration 16.0 mM was calculated from the titration

and then varied at concentration of 28.0, and 40.0 mM; nitric acid was used to adjust the pH to 9.0 under these concentrations. Better separation and good peak symmetry were obtained at 16.0 mM of NH_4OH, while baseline noise was observed with increasing concentrations as the moles of mobile ions increased which led to higher ionic strength in the buffer (Figure 2.10).[25]

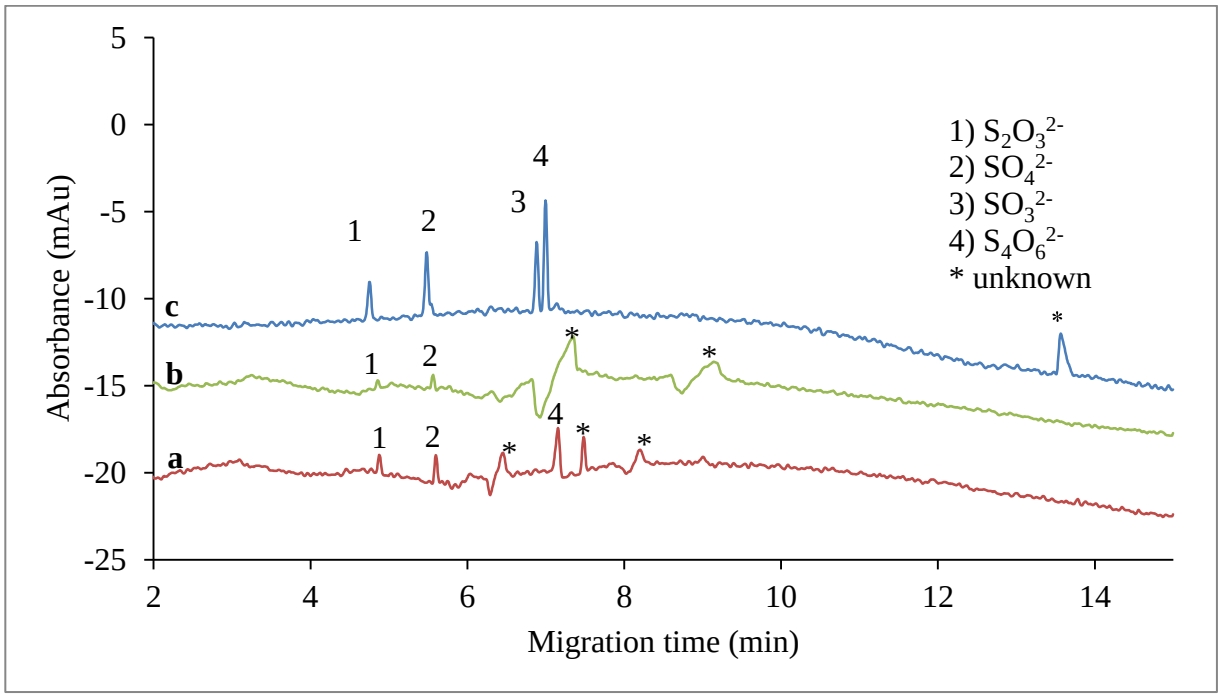

Figure 2.10. Mixture of $S_4O_6^{2-}$ 0.66 mM, SO_3^{2-} 0.40 mM. BGE: PMA 2.0 mM, NH_4OH: a) 40.0 mM, b) 28.0 mM, c) 16.0 mM, pH 9.0, DTPA 0.1 mM and HMOH 1.0 mM, CE conditions: capillary length 64.5 cm, injection 20 mbar for 5 s, applied voltage -30 kV at 25 °C. Spectra acquired at 360 nm with reference at 214 nm.

2.3.4 Influence of EOF

It was observed that sulfur-containing anion migration times could be very long because the EOF moves in the direction of the cathode with the bulk electrolyte flow and in the opposite direction to the electrophoretic migration of sample anions and away from the

detector. Thus, to determine the identity of anions, a reversed or reduced electroosmotic flow was applied to shorten the time of analysis.[13] For anions to move from the inlet to the outlet of the capillary, the anode should be located at the detector end (negative polarity), and will be detected first. EOF modifiers are used to reduce EOF and increase apparent electrophoretic mobilities for all sulfur species (shorten the time of separation), but they can also improve reproducibility and resolution of inorganic anions.[13,26]

EOF modifiers are usually cationic surfactants that are adsorbed to the silica capillary through electrostatic interaction by ionization of silanol groups (SiOH) on the surface of bare-fused silica. Deprotonation of the silanol groups on the silica surface is required to obtain a strong electrostatic attraction; this occurs at pH above 3. Consequently, as the pH increases the positive charge on the capillary surface increases because more surfactant adsorbs to the silica surface. The result is a surface with a net positive charge that greatly reduces or eliminates analyte-surface interaction as well as reducing or reversing the EOF as shown in Figure 1.3.[20,26]

Alkyl ammonium salts are the most common EOF modifiers used for the analysis of the inorganic anions, such as tetramethylammonium hydroxide (TMAOH), hexadecyltrimethylammonium bromide (CTAB) and hexamethonium hydroxide (HMOH). HMOH has higher solubility and lower tendency to form ion-pairs than the other EOF modifiers (Figure 2.11).[9,11,13,20] Therefore, it was chosen to achieve a good peak resolution, better peak symmetry as well as shorter analysis.[20] The HMOH concentration was varied (0.6, 0.8, and 1.0 mM) with a constant concentration of the PMA probe of 2.00 mM based on previous work done by Pappoe et al. (2014).[2,20] The EOF is reduced and the ions migration towards the detector will be faster with increasing

HMOH concentration. However, once the surface of the capillary is fully coated by the modifiers, the EOF will not be changed and an increased concentration of modifiers will negatively affect the separation or resolution of the analytes due to the formation of neutral ion-pairs between analyte anions or PMA as well as the excess of EOF modifier (HM^+).[1,9,11,20] Thus, the optimum concentration of HMOH was found to be 1.0 mM, with this concentration allowing for good separation with little impact on other performance characteristics (Figure 2.12).

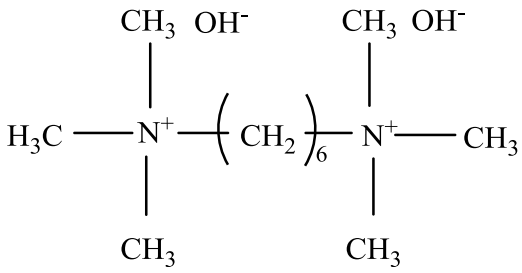

Figure 2.11. Hexamethonium hydroxide (HMOH).

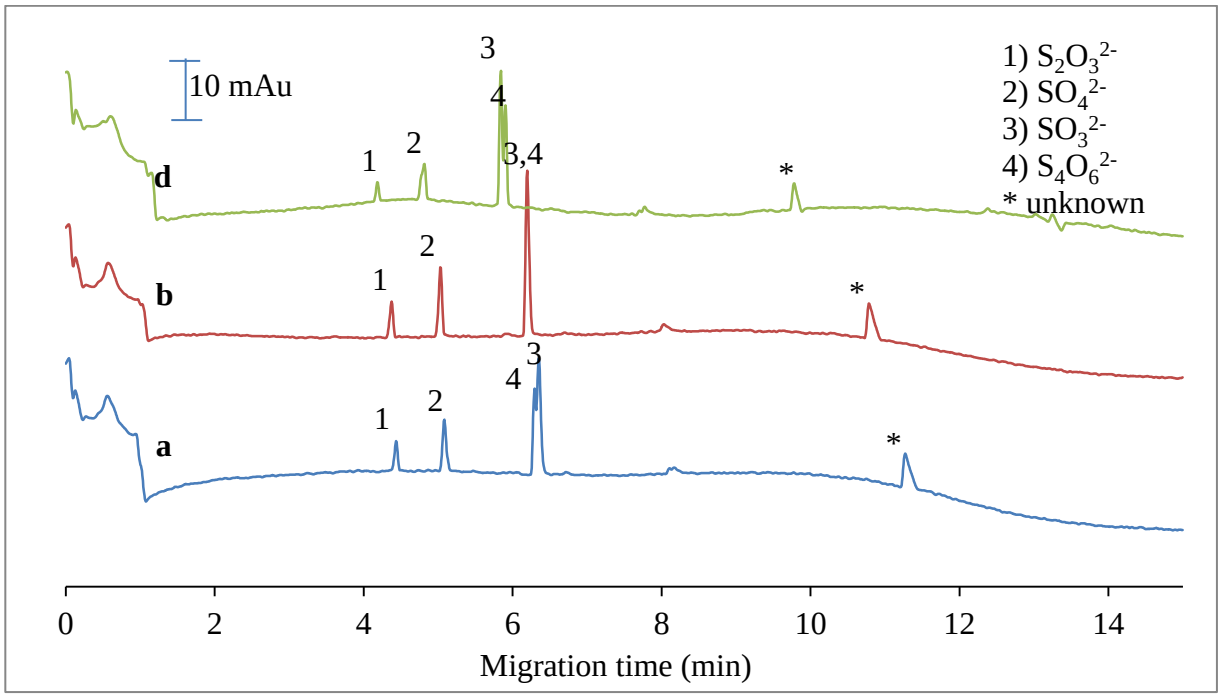

Figure 2.12. Mixture of $S_4O_6^{2-}$ 0.66 mM, SO_3^{2-} 0.40 mM, BGE: PMA 2.0 mM, adjusted to pH 9.0 with NH_4OH, DTPA 0.1 mM plus HMOH: a) 0.6 mM b) 0.8 mM c) 1.0 mM. CE conditions: capillary length 64.5 cm, injection 20 mbar for 5 s, applied voltage -30 kV at 25 °C. Spectra acquired at 360 nm with reference at 214 nm.

2.3.5 Capillary Temperature and Length

The capillary temperature was also optimized in this work as a lower temperature can reduce Joule heating and dispersion. The effect of temperature on the separation was examined at 15 °C and 25 °C. In this study, the optimum temperature was found to be 25 °C. At the lower temperature (15 °C), the viscosity is higher than at 25 °C which leads to a decrease in the mobility of the analytes and therefore an increase in migration time (Figure 2.13). The improvement in the peak shape and width was negligible because the longer migration times meant more time for dispersion related broadening. All further experiments were carried out at 25 °C.

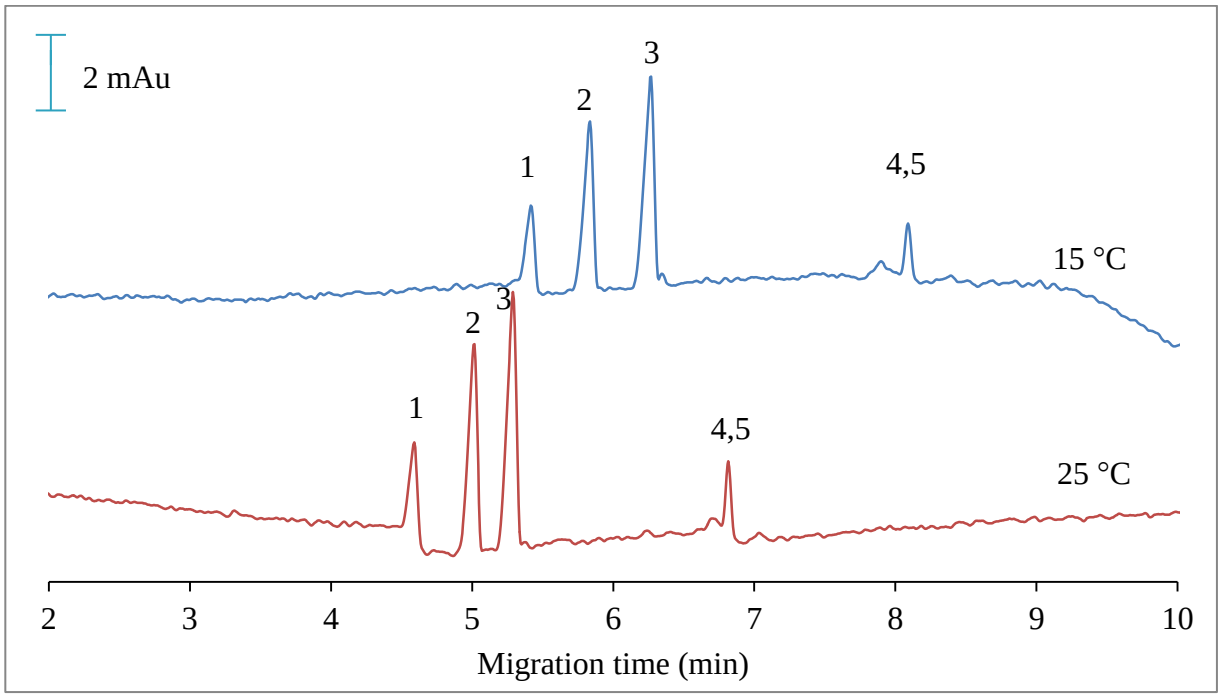

Figure 2.13. Mixture of 1) $S_2O_3^{2-}$ 0.20 mM, 2) Cl^- 0.86 mM, 3) SO_3^{2-} 0.35 mM, 4) $S_4O_6^{2-}$ 0.17 mM, 5) SO_3^{2-} 0.40 mM. BGE: PMA 2.0 mM, HMOH 0.8 mM, and adjusted to pH 8.0 with TEA, CE conditions: capillary length 64.5 cm, injection 20 mbar for 5 s, applied voltage -30 kV. Spectra acquired at 360 nm with reference at 214 nm.

Given that increasing the length of the capillary increases the number of theoretical plates and resolving power, but increases migration time and band broadening, capillary length was also optimized to achieve complete separation of sulfur anions in the shortest time. Capillary lengths were investigated for two lengths at 48.5 cm and 64.5 cm. Complete separation of a mixture of $S_2O_3^{2-}$, Cl^-, SO_4^{2-}, $S_4O_6^{2-}$ was achieved with 64.5 cm; this could not be attained with the shorter capillary (Figure 2.14).

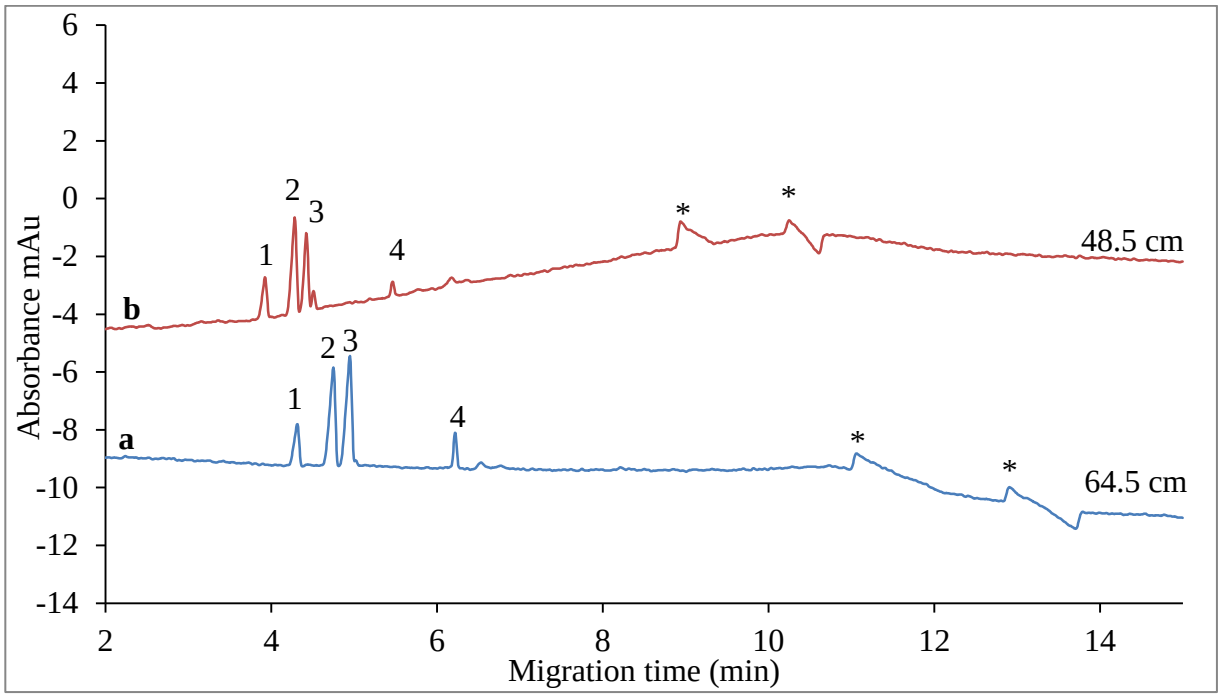

Figure 2.14. Mixture of 1) $S_2O_3^{2-}$ 0.20 mM, 2) Cl^- 0.86 mM, 3) SO_4^{2-} 0.35 mM, 4) $S_4O_6^{2-}$ 0.17 mM, * unknown. BGE (HMOH 0.8 mM, PMA 2.0 mM, and adjusted to pH 8.0 with TEA, DTPA 0.1 mM), CE conditions: capillary length a) 64.5cm, b) 48.5cm, injection 20 mbar for 5 s, applied voltage -30 kV at 25 °C.

2.5 Analysis of a Real Samples

The optimum composition of the BGE was 6.0 mM PMA and 1.0 mM HMOH adjusted to pH 9.0 with 16.0 mM NH_4OH, where all were dissolved in 0.10 mM of DTPA. Separation of $S_2O_3^{2-}$, SO_4^{2-}, SO_3^{2-}, and $S_4O_6^{2-}$ in the presence of chloride was achieved within 7 minutes (Figure 2.15) at a potential of -30 kV. The order of migration was estimated by the mass-to-charge ratio. However, since the trend in hydrodynamic ratio can diverge from the mass trend, positions were confirmed by spiking with individual standards. Although sulfate and thiosulfate have the same charge and mass, thiosulfate migrates faster as it has a smaller hydration sphere.

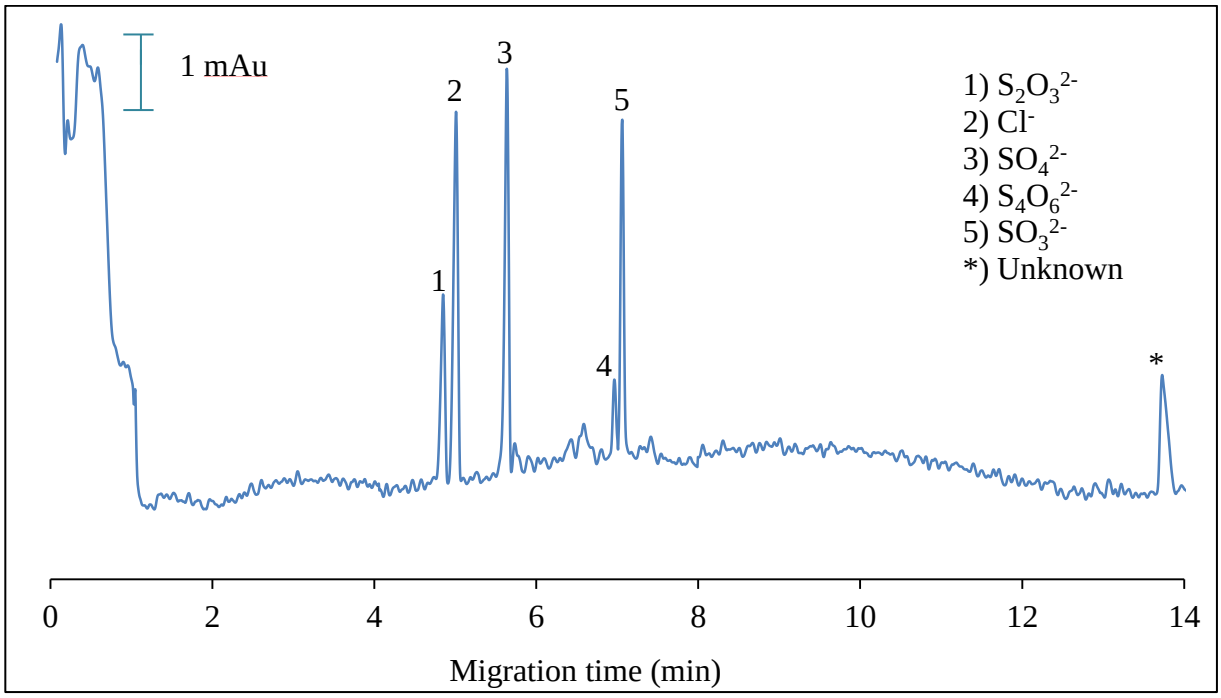

Figure 2.15. Mixture of 1) $S_2O_3^{2-}$ 0.20 mM, 2) Cl^- 0.86 mM, 3) SO_4^{2-} 0.35 mM, 4) $S_4O_6^{2-}$ 0.17 mM, 5) SO_3^{2-} 0.40 mM. BGE: PMA 6.0 mM, HMOH 1.0 mM, NH_4OH 16.0 mM, pH 9.0, DTPA 0.1 mM, CE conditions: capillary length 64.5 cm, injection 20 mbar for 5 s, applied voltage -30 kV. Spectra acquired at 360 nm with reference at 214 nm.

All sulfur species were well-resolved in a standard solution with good peak intensity using the final BGE composition and instrument parameters of indirect UV-detection at 360 nm with a reference at 214 nm. The migration order was thiosulfate, chloride, sulfate, bisulfide, sulfite, and tetrathionate. However, when the undiluted produced water was injected, it was impossible to resolve thiosulfate from the high concentration of Cl^- naturally present in real samples (Figure 2.16). This problem was observed previously by Chen et al. (2003).[1]

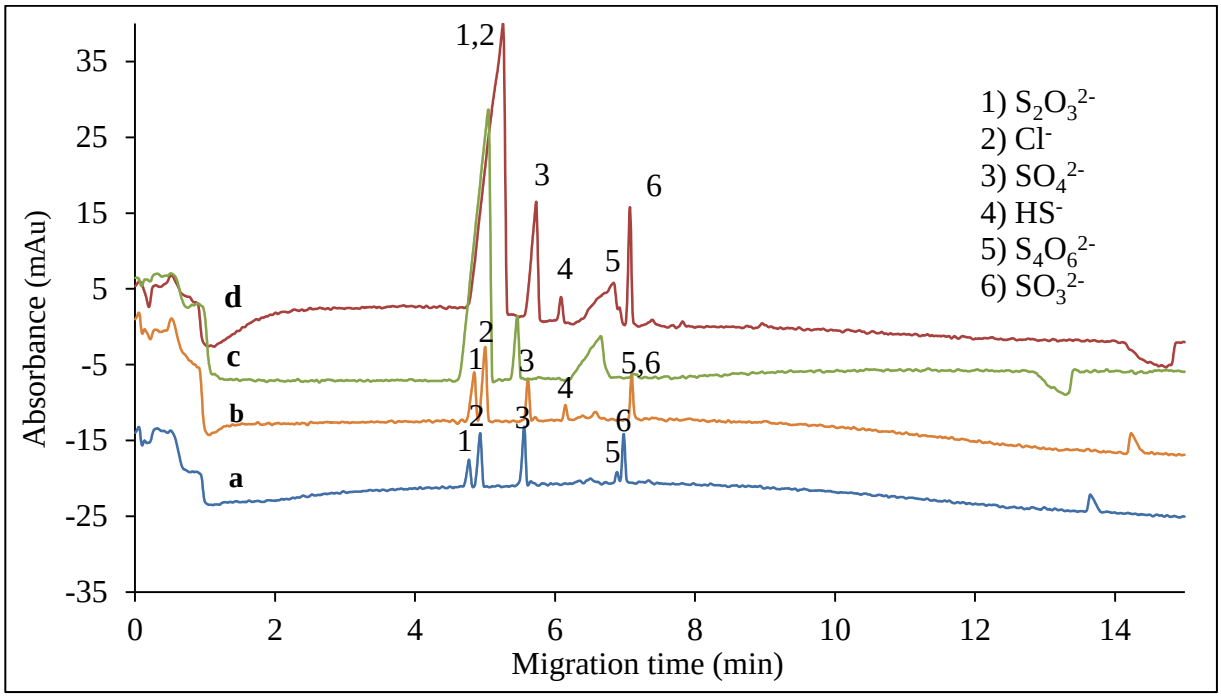

Figure. 2.16. a) mixture of $S_2O_3^{2-}$ 0.20 mM, Cl^- 0.86 mM, SO_4^{2-} 0.35 mM, $S_4O_6^{2-}$ 0.17 mM, and SO_3^{2-} 0.40 mM, b) S^{2-} 0.64 mM plus mixture (a), c) produced water, d) produced water spiked with SO_3^{2-} 1.59 mM, SO_4^{2-} 1.41 mM, $S_2O_3^{2-}$ 0.81 mM, $S_4O_6^{2-}$ 0.66 mM, Cl^- 3.42 mM, S^{2-} 2.56 mM.

2.6 Development of CE with Direct UV Detection to Overcome Matrix Interferences for Thiosulfate

Since $S_2O_3^{2-}$, S^{2-}, HS^- and $S_4O_6^{2-}$ have relatively strong UV absorptivity, and Cl^- is non-absorbing UV, as are SO_4^{2-} and SO_3^{2-} (Figure 2.2, a, b), it is possible to use the more selective direct detection mode to determine the thiosulfate in produced water. However, this required that a new BGE be optimized. Alkaline conditions are still required to keep sulfur-containing species stable, hence ammonium hydroxide (16.0 mM) was used and adjusted to pH 9.0 with formic acid (CH_2O_2, pK_a=3.75). No chromophoric probe was used but hexamethonium hydroxide HMOH (1.0 mM) was still needed to reduce EOF

and allow for the detection of all anions with good peak resolution, better peak symmetry, as well as shorter analysis time. Because Cl^-, SO_4^{2-} and SO_3^{2-} exhibit no absorbance, they do not interfere with the detection of sulfur anions (Figure 2.17) and the UV-Vis spectra (Figure 2.3 b). However, SO_3^{2-} shows in Figure 2.17 (d) as a peak around 6 minutes which indicated a further reaction inside the capillary. This will be explained in Chapter 4, Section (4.3). There is a decrease in the pH of the electrolyte during the time of the analysis due to the redox reaction inside the capillary which transforms SO_3^{2-} into bisulfite HSO_3^- and further to SO_2 that has an absorbance.[27]

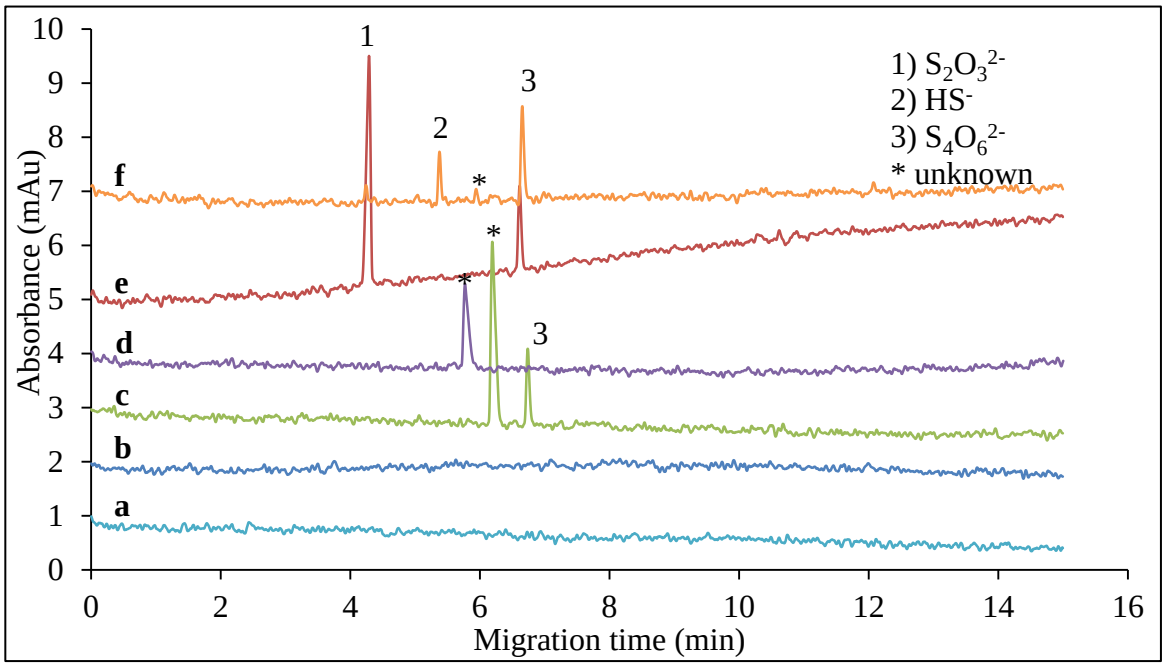

Figure. 2.17. a) SO_4^{2-} 1.41 mM, b) Cl^- 3.42 mM, c) $S_4O_6^{2-}$ 0.66 mM, d) SO_3^{2-}1.59 mM, e) $S_2O_3^{2-}$ 0.81 mM, f) S^{2-} 2.56 mM. BGE: 1.0 mM HMOH, 16.0 mM NH4OH, CH_2O_2, pH 9.0. CE conditions: capillary length 64.5 cm, injection 20 mbar for 5 s. applied voltage -30 kV, temperature 25 °C. Spectra acquired at 214 nm with reference at 360 nm

Figure 2.18 shows the electropherograms obtained for standard solutions and for 10-fold diluted produced water by direct UV detection. Figure 2.19 shows that both direct and indirect methods were successfully applied to the analysis of sulfide and thiosalt species in produced water, and effectively surmounted the challenges posed by the high salinity of the produced water.

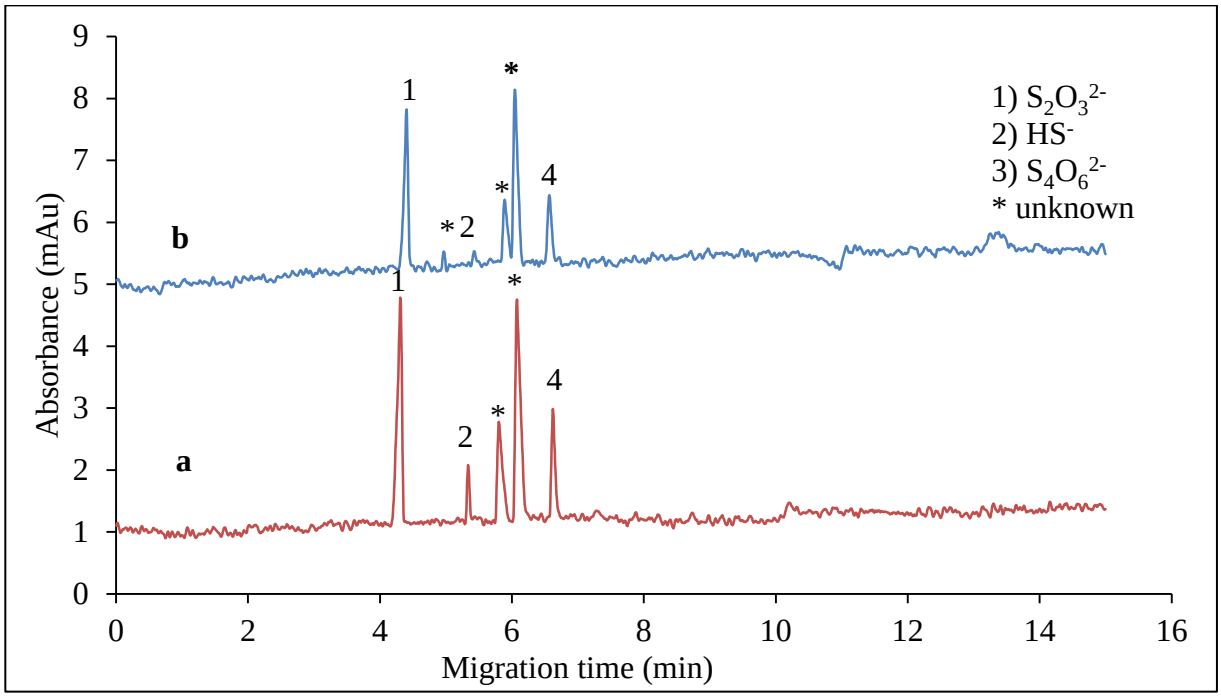

Figure. 2.18. Direct CE analysis of: a) standard mix of SO_3^{2-} 1.59 mM, SO_4^{2-} 1.41 mM, $S_2O_3^{2-}$ 0.81 mM, $S_4O_6^{2-}$ 0.66 mM Cl^- 3.42 mM, S^{2-} 2.56 mM, b) produced water. BGE: 1.0 mM HMOH, 16.0 mM NH_4OH, CH_2O_2, pH 9.0. CE conditions: capillary length 64.5 cm, injection 20 mbar for 5 s. applied voltage -30 kV, temperature 25 °C. Spectra acquired at 214 nm with reference at 360 nm.

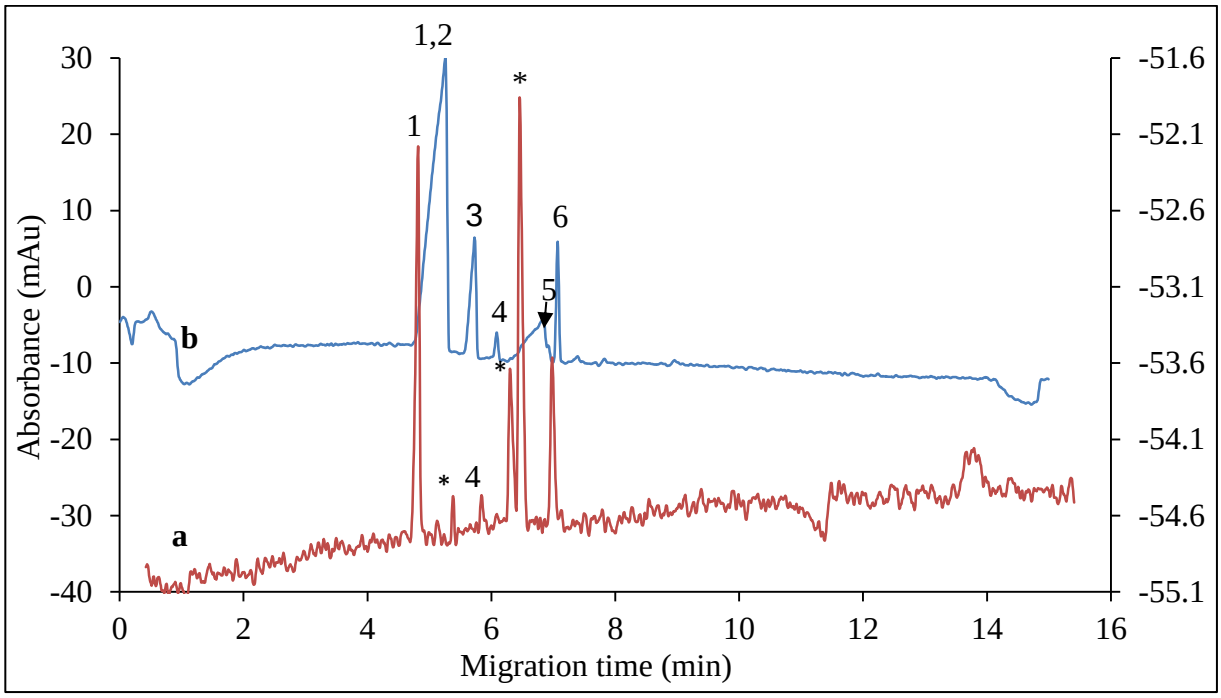

Figure. 2.19. Produced water with 1) $S_2O_3^{2-}$ 0.81 mM, 2) Cl^- 3.42 mM 3) SO_4^{2-} 1.41 mM, 4) HS^- 2.56 mM, 5) $S_4O_6^{2-}$ 0.66 mM, 6) SO_3^{2-} 1.59 mM. BGE: a) direct method: 1.0 mM HMOH, 16.0 mM NH_4OH, CH_2O_2, pH 9.0, b) indirect method: 1.0 mM HMOH, 16.0 mM NH_4OH, 6.0 mM PMA, pH 9.0. Spectra acquired at 214 nm with reference at 360 nm.

2.7 Linearity of Method, Sensitivity, and LOD Determination

The linearity, detection limit and reproducibility for analysis by the CZE indirect method are listed in Table 2.1. Calibration curves have been used to establish the relationship between the concentration and the electrophoretic peak area. Each standard sample was injected in triplicate and the standard deviation of the peak areas and migration times was determined. The integrated areas of the peaks for thiosulfate, chloride, sulfate, bisulfide, and tetrathionate were found to exhibit excellent linear correlations over the concentration range of 0.5 mg/L to 25 mg/L. The correlation coefficient was always above 0.99 (Figure 2.20). The limit of detection (LOD) values were obtained at signal to noise (S/N) ratios of

3 by sequential dilution of thiosalt mixtures until the S/N value of the peak of interest reached 3, while the limit of quantitation (LOQ) is 10 times the S/N ratio. The data showed that electrophoretic separations of these analytes could be carried out with high reproducibly and accurately. However, the indirect method failed to identify $S_2O_3^{2-}$ in high salinity of produced water. Hence, the direct method was investigated in this work to solve the interference problem between $S_2O_3^{2-}$ and the high concentration of Cl^- presented in the produced water. The direct method successfully separated $S_2O_3^{2-}$ with excellent linearity over the range 0.5 mg/L to 25 mg/L and correlation coefficient better than 0.99 (Figure 2.21). The detection limit for $S_2O_3^{2-}$, HS^-, $S_4O_6^{2-}$ ranged from 0.059 to 0.465 mg/L, and LOQ from 0.316 to 1.549 mg/L (Table 2.2).

Both the indirect and direct methods can be used to identify $S_2O_3^{2-}$, HS^-, and $S_4O_6^{2-}$. However, the direct method is required to detect $S_2O_3^{2-}$ and eliminate non-absorbing Cl^- interference in real samples and it was also preferable to detect $S_4O_6^{2-}$ because of the lower limit of detection of this method compared to that of the indirect detection since the molar absorptivity was closed for PMA and $S_4O_6^{2-}$. The limit of detection for HS^- in both methods was high because it was a weak acid.

Table 2.1. Figures of Merit for Indirect Analysis.

	Coefficient of regression (R^2)	LOD (mg/L) (n=3)	LOQ (mg/L) (n=3)
Cl^-	0.9994	0.0361	0.120
SO_4^{2-}	0.9986	0.0403	0.134
$S_2O_3^{2-}$	0.9995	0.110	0.366
HS^-	0.9978	0.354	1.181
$S_4O_6^{2-}$	0.9951	0.144	0.479

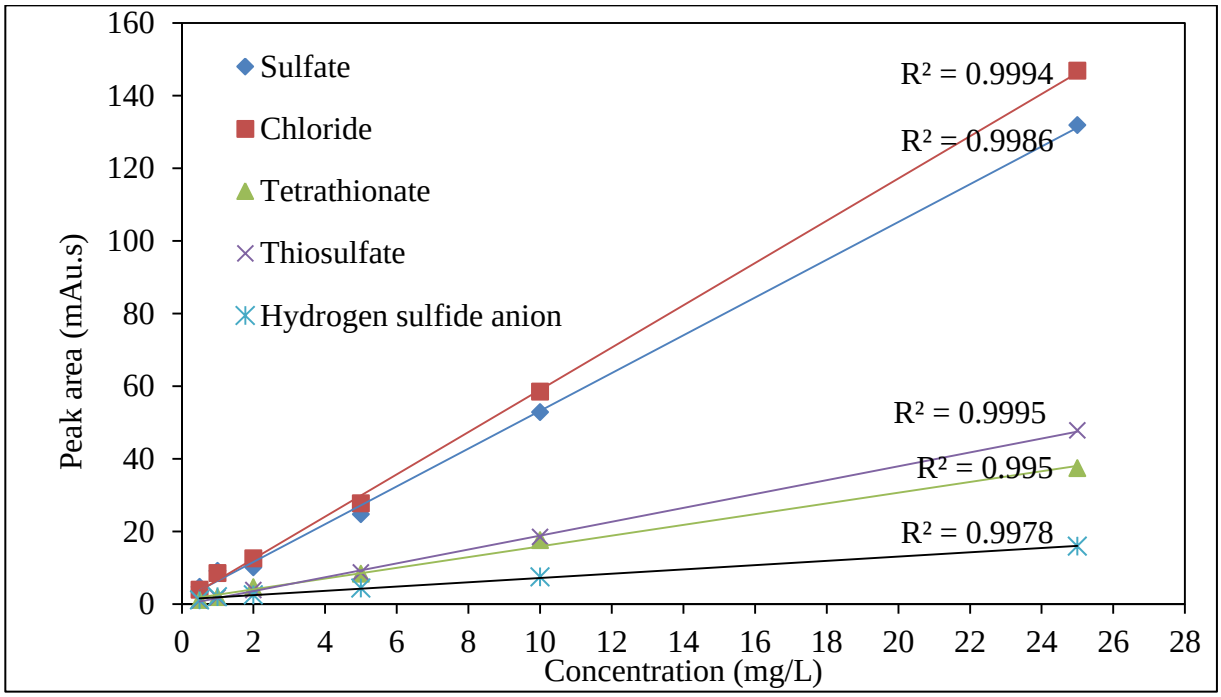

Figure. 2.20. Standard calibration curves obtained from indirect analysis of a mixture of standards (HS^-, $S_4O_6^{2-}$, $S_2O_3^{2-}$, SO_4^{2-}, Cl^-) in concentrations of 0.5, 1.0, 2.0, 5.0, 10.0, 25.0 mg/L each.

Table 2.2. Figures of Merit for Direct Analysis.

	Coefficient of regression (R^2)	LOD (mg/L) (n=3)	LOQ (mg/L) (n=3)
$S_2O_3^{2-}$	0.9997	0.059	0.197
HS^-	0.9995	0.465	1.549
$S_4O_6^{2-}$	0.9989	0.095	0.316

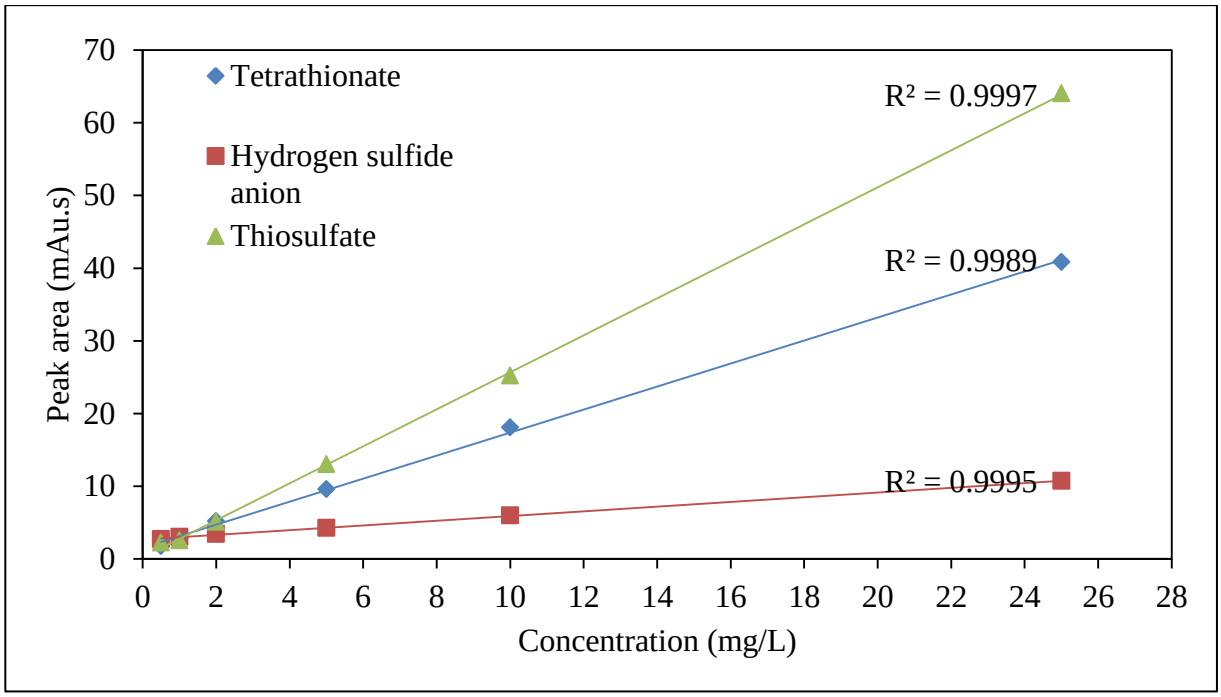

Figure. 2.21. Standard calibration curves obtained from direct analysis of a mixture of standards ($S_2O_3^{2-}$, HS^-, $S_4O_6^{2-}$) in concentrations of 0.5, 1.0, 2.0, 5.0, 10.0, 25.0 mg/L each.

2.8 Conclusions

When considering the aspects indicated above, there is now a solid basis of knowledge and techniques available for quantitative CZE of sulfur-containing anions. By combining indirect and direct methods into a single analytical strategy, a sensitive, selective and reliable methodology was achieved that features complete separation of hydrogen sulfide (as HS^-), sulfate (SO_4^{2-}), sulfite (SO_3^{2-}), and thiosalts (thiosulfate ($S_2O_3^{2-}$), tetrathionate ($S_4O_6^{2-}$)) in produced water/reservoir water. The use of a stabilizing agent (DTPA) and purging samples with nitrogen was required to minimize analyte degradation as the sulfide and thiosalt species are easily oxidized by impurities and air. Optimization of the indirect BGE involved study of several parameters including concentration and nature of chromophoric probe (PMA), concentration of EOF modifier (HMOH), nature and pH of the base system and indirect UV detection at λ_{max}= 214 nm. Conversely, the BGE for direct detection was more straight forward requiring only optimization of the EOF modifier (HMOH), buffer system (pH 9.0) adjusted with formic acid, and direct UV detection at λ_{max}= 214 nm. The optimized methods were successfully applied to the analysis of sulfide and thiosalt species in reservoir samples, and solved the challenges presented by the high chloride concentration in the produced water.

2.9 References

(1) Chen, Z.; Naidu, R. *Int. J. Environ. Anal. Chem.* **2003**, *83* (9), 749–759.

(2) O'Reilly, J. W.; Dicinoski, G. W.; Shaw, M. J.; Haddad, P. R. *Anal. Chim. Acta* **2001**, *432* (2), 165–192.

(3) Petre, C. F.; Larachi, F. *J. Sep. Sci.* **2006**, *29*, 144–152.

(4) Kellogg, W. W.; Cadle, R. D.; Allen, E. R.; Lazrus, A. L.; Martell, E. A. *Science* **1972**, *175* (4022), 587–596.

(5) Hissner, F.; Mattusch, J.; Heinig, K. *J. Chromatogr. A* **1999**, *848* (1–2), 503–513.

(6) Ericka L. Barrett and Marta A. Clark. *Microbiol. Rev.* **1987**, *51* (2), 192–205.

(7) Jiang, J.; Chan, A.; Ali, S.; Saha, A.; Haushalter, K. J.; Lam, W.-L. M.; Glasheen, M.; Parker, J.; Brenner, M.; Mahon, S. B.; Patel, H. H.; Ambasudhan, R.; Lipton, S. A.; Pilz, R. B.; Boss, G. R. *Sci. Rep.* **2016**, *6* (October 2015), 20831.

(8) Timerbaev, A. R.; Dabek-Zlotorzynska, E.; van den Hoop, M. a. G. T. *Analyst* **1999**, *124* (6), 811–826.

(9) Padarauskas, A.; Paliulionyte, V.; Ragauskas, R.; Dikcius, A. *J. Chromatogr. A* **2000**, *879* (2), 235–243.

(10) Haddad, P. R. *J. Chromatogr. A* **1997**, *770* (1–2), 281–290.

(11) Words, K. *Chromatographia* **2002**, 51, 723–728.

(12) Haddad, P. R.; Doble, P.; Macka, M. *J. Chromatogr.* **1999**, *856*, 145–177.

(13) Safizadeh, F.; Larachi, F. *Instrum. Sci. Technol.* **2014**, *42* (3), 215–229.

(14) Yilmaz, Ü. T.; Somer, G. *Anal. Chim. Acta* **2007**, *603* (1), 30–35.

(15) Guenther, E. A.; Johnson, K. S.; Coale, K. H. *Anal. Chem.* **2001**, *73* (14), 3481–3487.

(16) Sullivan, J.; Douek, M. *J. Chromatogr. A* **2004**, *1039* (1–2), 215–225.

(17) Hughes, M. N.; Centelles, M. N.; Moore, K. P. *Free Radic. Biol. Med.* **2009**, *47* (10), 1346–1353.

(18) Zhang, H.; Jeffrey, M. I. *Inorg. Chem.* **2010**, *49* (22), 10273–10282.

(19) Laine, P.; Matilainen, R. *Anal. Bioanal. Chem.* **2005**, *382* (7), 1601–1609.

(20) Pappoe, M.; Bottaro, C. S. *Anal. Methods* **2014**, *6* (23), 9305–9312.

(21) Motellier, S.; Gurdale, K.; Pitsch, H. *J. Chromatogr. A* **1997**, *770* (1–2), 311–319.

(22) De Carvalho, L. M.; Schwedt, G. *J. Chromatogr. A* **2005**, *1099* (1–2), 185–190.

(23) Vongporm, Y.; A. Thiosalt behaviour in aqueous media, Memorial University of Newfoundland, **2008**, Vol. 1.

(24) Zopfi, J.; Ferdelman, T.G.; Fossing, H. *Geological Society of America Special* **2004**, 379, 97–116.

(25) Persat, A.; Suss, M. E.; Santiago, J. G. *Lab Chip* **2009**, *9* (17), 2454–2469.

(26) Revermann, T.; Götz, S.; Künnemeyer, J.; Karst, U. *Analyst* **2008**, *133* (2), 167–174.

(27) Hawe, E.; Fitzpatrick, C.; Chambers, P.; Dooly, G.; Lewis, E. *Sensors Actuators, A Phys.* **2008**, *141* (2), 414–421.

Chapter 3. Reactivity of Sulfite and Tetrathionate and the Effect of Sulfide Presence

3.1 Introduction

The chemistry of sulfide and sulfur oxygen anions is complex and easily influenced by changes in the system conditions; most importantly pH and temperature changes can shift equilibria and speciation. Furthermore, the presence of oxygen, metals and microorganisms can cause an additional speciation.[1,2] The complexity of sulfur species chemistry and reactions is due to the possibility of multiple reaction pathways and products. Contributing to the challenges and ambiguity of the systems is that reaction mechanisms change with the reaction conditions (e.g., changes in pH) and can generate complex mixtures of metastable sulfur species. For example, thiosulfate is most reactive in acidic conditions (pH 2), while tetrathionate decomposes when the pH goes above 9, though they are both relatively stable between pH 2 and pH 9 for temperatures up to 30 ^{o}C.[1,3] Sulfite stability is higher in basic media than in acidic.[4] Hydrogen sulfide is an acid with pK_a values of 6.9 and 14, so the extent of ionization of hydrogen sulfide (HS^-) and sulfide anion (S^{2-}) varies with pH. Tetrathionate and sulfite can react not only with explicit oxidants like Fe^{3+}, but also with each other, making their reactivity mechanisms particularly complicated.[5,6] According to the reactions proposed in the literature, a good understanding of the chemistry of the thiosulfate, sulfide, and polythionate is critical for control and treatment of reservoir souring. With multiple reactions pathways, it is difficult to separate and quantify sulfur species accurately. Since the composition of these mixtures can change relatively quickly, fast separation technologies are required to determine the relevant species simultaneously. Where the classical titration methods are

quite time-consuming and difficult to employ in the presence of multiple similar species, capillary electrophoresis (CE) has advantages in separation efficiency and speed, tolerance to sample matrices (especially high pH), cost of consumables, and selectivity. Furthermore, because the separation does not rely on any interactions with a solid-phase, as with traditional separation methods, CE is increasingly being used in studies of the sulfur species and their reactions.[7,8] In this work, an attempt has been made to study the complex relationships in mixtures of sulfur anions, with interconversion occurring spontaneously in weakly basic conditions over time.

3.2 Instrumentation

All experiments were performed with the Agilent 7100^{3D} CE System (Agilent Technologies Canada Inc., Mississauga, ON) equipped with a diode array UV-Vis detector. Separation occurred inside bare fused- silica capillaries (50 μm i.d. (internal diameter)) were obtained from MicroSolv Technology Corporation (NJ, USA) and were accurately cut to the desired length (64.5 cm). A MicroSolv Window Maker™ (N.J. USA) was used to burn the external polyimide coating from the capillaries at 8.5 cm to create a detection window and at the last 2 mm of the ends. Indirect UV detection at 360 nm with a reference wavelength at 214 nm (to invert the negative peaks) was employed. Corrected peak areas, peak widths and heights, and migration times were calculated using Agilent OpenLAB Chromatography Data System (CDS) ChemStation. Initial capillary conditioning and conditioning between consecutive runs are the same as in Chapter 2. Samples were injected hydrodynamically by overpressure 20 mbar for 5 s from the cathodic compartment inlet. A negative potential (-30 kV) for the separation was

ramped up to a constant potential over 1 minute. The temperature of the capillary compartment was maintained at 25 °C for all experiments.

3.3 Chemicals and Reagents

All chemicals used for this work were of analytical grade and purchased from Sigma-Aldrich unless otherwise noted. Pyromalitic acid PMA in pyromallitate form was used as a chromophoric probe in indirect CZE to provide a background signal and improve detection sensitivity for non- absorbing anions in the direct CE mode. As the electroosmotic flow (EOF) increases with the pH, in neutral and basic conditions a modifier, hexamethanium hydroxide (HMOH) was introduced to the running buffer solution to reduce EOF flow and decrease separation time. BIS-TRIS (BIS[2-hydroxyethyliminotris[hydroxymethyl]methane) >98% was used to control pH for pH 7.0 runs, triethanolamine (TEA) for pH 8.0, and ammonium hydroxide (NH_4OH) for pH 9.0. CE grade sodium hydroxide solution (1.0 M) was purchased from Agilent (Agilent Technologies Canada Inc., Mississauga, ON). All water used in this work was optima LC/MS water (suitable for UHPLC-UV, Fisher Chemical, UK). Stock solutions of 1000 mg/L of sodium thiosulfate ($Na_2S_2O_3$ > 99.9%), sodium tetrathionate ($Na_2S_4O_6$ > 99.9%), sodium sulfide (Na_2S), sodium hydrosulfide hydrate ($HNaS.xH_2O$) were prepared fresh daily in nitrogen- bubbled deoxygenated LC water containing a stabilizing agent, diethylenetriamine-pentacetic acid (DTPA > 99%) at 0.1 mM and kept in amber bottles at 4 °C, except when being analyzed. [9,10] All solutions including standards, samples, and background electrolytes were deoxygenated with nitrogen and DTPA added to limit oxidation by oxygen and other impurities (e.g., iron(III) or

copper(II)).[10] At this concentration, DTPA does not show absorption.[11] Solutions were also degassed by sonication and filtered with a 0.22 µm nylon syringe filter (Canadian Life Science, ON) prior to CE analysis. In the indirect CZE method, the running buffers were composed of 6.0 mM PMA and 1.0 mM HMOH and titrated with NH_4OH to pH 9.0 as was explained in detail in Chapter 2.[10]

3.4 Reaction Pathway Considerations

3.4.1 Reactions Involving Thiosulfate

Thiosulfate is reactive in acidic media, and the reactivity increases with temperature. While stable in neutral and alkaline aqueous systems at temperatures below 70 °C, it decomposes above 70 °C to produce sulfate.[5,13] Thiosulfate can be one of the oxidation products of sulfide in the presence of the air and sulfite, where sulfide as HS^- reacts as shown in the following equation:[14]

$$HS^- + SO_3^{2-} + 0.5O_2 \longrightarrow S_2O_3^{2-} + OH^- \quad (3.1)$$

Thiosulfate disproportionation is a key process in the sulfur cycle.[14] In a basic solution, thiosulfate can react in the absence of explicit oxidizing agents to form polythionates, mainly tetrathionate and trithionate (Eq. 3.2). If additional oxidizing agents are present, such as oxygen (O_2) or by copper(II) or iron(III) in these conditions, thiosulfate can undergo complete oxidation to sulfate (Eq. 3.3): [3,5,15] [16,17]

$$5S_2O_3^{2-} + 6OH^- \longrightarrow 2S_3O_6^{2-} + S_4O_6^{2-} + 3H_2O \quad (3.2)$$

$$S_2O_3^{2-} + 2O_2 + 2OH^- \longrightarrow 2SO_4^{2-} + H_2O \quad (3.3)$$

Thiosulfate can be a byproduct in almost all the solutions containing polythionate, either as an impurity or as generated from other reactions.[5] It is notable that polythionates start to decompose and reduce to regenerate thiosulfate under similar alkaline conditions.[5,15] For example, thiosulfate, in addition to trithionate, is the product from a sulfitolysis reaction as sulfite reacts with tetrathionate when they exist together:

$$S_4O_6^{2-} + SO_3^{2-} \longrightarrow S_3O_6^{2-} + S_2O_3^{2-} \quad (3.4)$$

Thiosulfate simultaneously acts as a catalyst in the rearrangement reaction for the production of polythionates and other S-compounds in the aqueous system as shows in the general disproportionation reaction:[1,5,15,18]

$$S_xO_6^{2-} + S_2O_3^{2-} \rightleftharpoons S_{x+1}O_6^{2-} + SO_3^{2-} \quad (3.5)$$

For example, the tetrathionate rearrangement reaction is catalyzed by thiosulfate to generate sulfite and pentathionate followed by their further reactions:[3,5]

$$S_4O_6^{2-} + S_2O_3^{2-} \rightleftharpoons S_5O_6^{2-} + SO_3^{2-} \quad (3.6)$$

$$2S_5O_6^{2-} + 4S_2O_3^{2-} \longrightarrow 3S_4O_6^{2-} + S_6O_6^{2-} \quad (3.7)$$

Zhang and Jeffrey (2010) showed that $S_2O_3^{2-}$ can also form from $S_3O_6^{2-}$ hydrolyzation:[5]

$$2S_3O_6^{2-} + 6OH^- \longrightarrow S_2O_3^{2-} + 4SO_3^{2-} + 3H_2O \quad (3.8)$$

$$S_3O_6^{2-} + H_2O \longrightarrow S_2O_3^{2-} + SO_4^{2-} + 2H^+ \quad (3.9)$$

Moreover, pentathionate decomposition in alkaline media also produced thiosulfate:[5,15,18]

$$2S_5O_6^{2-} + 6OH^- \longrightarrow 5S_2O_3^{2-} + 3H_2O \quad (3.10)$$

3.4.2 Reactions Involving the Tetrathionate and Sulfite Ions

A mixture of sulfur-oxygen species show a complex relationship in which the concentration in one species can disrupt equilibrium for a host of other species. For example, polythionate as tetrathionate decomposes to trithionate and pentathionate when the pH goes above 9, while it is relatively stable between pH 2 and pH 9 as shown in the overall reactions:[5,15]

$$2S_xO_6^{2-} \longrightarrow S_{x-1}O_6^{2-} + S_{x+1}O_6^{2-} \quad (3.11)$$

$$2S_4O_6^{2-} \longrightarrow S_3O_6^{2-} + S_5O_6^{2-} \quad (3.12)$$

Either of the following reactions can describe the overall decomposition of tetrathionate in alkaline solutions:

$$4S_4O_6^{2-} + 6OH^- \longrightarrow 2S_3O_6^{2-} + 5S_2O_3^{2-} + 3H_2O \quad (3.13)$$

$$2S_4O_6^{2-} + 6OH^- \longrightarrow 2SO_3^{2-} + 3S_2O_3^{2-} + 3H_2O \quad (3.14)$$

$$4S_4O_6^{2-} + 10OH^- \longrightarrow 2SO_4^{2-} + 7S_2O_3^{2-} + 5H_2O \quad (3.15)$$

Eq. 3.13 is the predominant reaction in weakly alkaline solutions where the pentathionate is not observed as it is not a stable end product due to its fast alkaline degradation.[1,5,6,15,16] Relative amounts of sulfite were formed during tetrathionate decomposition, and subtle amounts of sulfate were formed with increasing pH as shown in (Eq. 3.14). Trithionate

further hydrolyzes to $S_2O_3^{2-}$ and SO_3^{2-} or SO_4^{2-} in basic condition as in equations (3.8) and (3.9).[5]

Tetrathionate also undergoes a complicated rearrangement reaction that might be catalyzed by thiosulfate (Eq. 3.5).[1,3,5,15,18] Existing tetrathionate and sulfite together cause a reaction, to produce thiosulfate and trithionate (Eq. 3.4) (Figure 3.1).

According to the reactions proposed in the literature, tetrathionate is the only species that does not react directly to form sulfate. Therefore, the tetrathionate reaction must go to either thiosulfate, sulfite or trithionate, and or pentathionate before completing its oxidation.[5,15,13]

3.4.3 Reactions Involving Hydrogen Sulfide

Hydrogen sulfide is the predominate species at pH <6, while dissolved hydrogen sulfide (HS^-) is the dominant sulfur species at the pH >7. As this work was preformed under basic conditions, the predominant species was therefore HS^-. Bisulfide can react with other sulfur species. For example, sulfite can react with HS^- to form thiosulfate:

$$HS^- + SO_3^{2-} + 0.5O_2 \longrightarrow S_2O_3^{2-} + OH^- \quad (3.16)$$

Elemental sulfur can also be produced from the decomposition of HS^-:

$$HS^- \longrightarrow S\downarrow + H^+ + 2e^- \quad (3.17)$$

Elemental sulfur reacts with sulfite and sulfide to form thiosulfate, tetrathionate, also polysulfide as HS_n^-:

$$S + SO_3^{2-} \longrightarrow S_2O_3^{2-} \quad (3.18)$$

$$2S + 2SO_3^{2-} \longrightarrow S_4O_6^{2-} \quad (3.19)$$

$$(n\text{-}1)S + HS^- \longrightarrow HS_n^- \quad (3.20)$$

The bisulfide anion can also oxidize rapidly in the presence of oxygen, or other contaminants such as Fe(III) and Cu(II) in the samples:[10,14]

$$2HS^- + O_2 \longrightarrow 2S + 2OH^- \quad (3.21)$$

$$2HS^- + Fe^{3+} \longrightarrow 2Fe^{2+} + 2H^+ + S\downarrow \quad (3.22)$$

$$(n\text{-}1)\,S + S^{2-} \longrightarrow S_n^{2-} \quad (3.23)$$

Polysulfides (HS_n^-, S_n^{2-}) are not stable in the presence of oxygen and rapidly decompose to thiosulfate and elemental sulfur.[14]

Bisulfide can also oxidize to form sulfate as the overall reaction:

$$HS^- + 2O_2 \longrightarrow SO_4^{2-} + H^+ \quad (3.24)$$

Sulfite is usually the first product formed from the oxidation of sulfide:

$$HS^- + 1.5O_2 \longrightarrow HSO_3^- \quad (3.25)$$

The sulfite is formed then it oxidizes rapidly to form a sulfate that is commonly observed during sulfide oxidation experiments:[14]

$$SO_3^{2-} + 0.5O_2 \longrightarrow SO_4^{2-} \quad (3.26)$$

3.5 Results and Discussion

The chemistry of sulfur species in an aqueous mixture can be very complex. Sulfur species composition changes over time due to redox and nucleophilic displacement reactions in the mixture.[12] In this study, the focus has been on the transformation of the sulfur species over the time period relevant to analysis. Thiosulfate, chloride, sulfate, bisulfide, sulfite and tetrathionate were identified by comparing their migration time to that of a standard, and the peak areas are proportional to the various species concentrations at the time of injection. Once the individual standards are mixed, reactions begin to occur. Concentrations of sulfate and thiosulfate were observed in the first run, which was initiated 15 minutes after mixing, even though only sulfite and tetrathionate standards were present in the stock solutions (Figure 3.1).

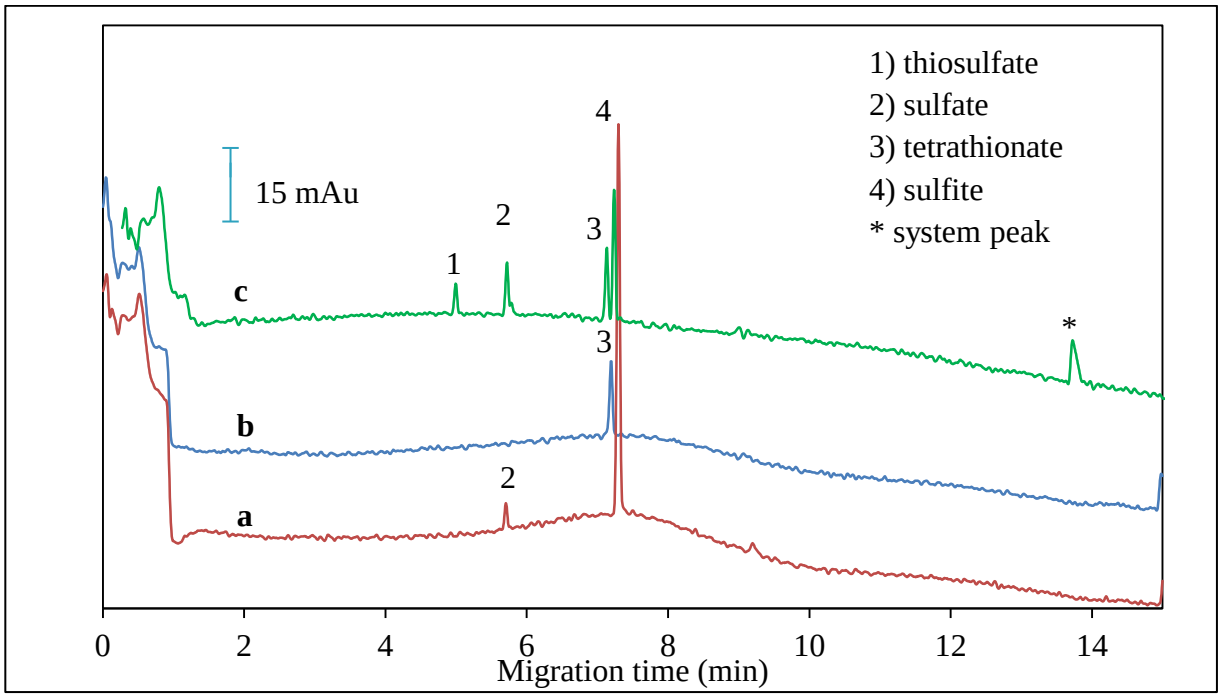

Figure. 3.1. a) SO_3^{2-} 1.59 mM, b) $S_4O_6^{2-}$ 0.66 mM, c) mixture of $S_4O_6^{2-}$ 0.66 mM and SO_3^{2-} 0.40 mM. BGE (PMA 6.0 mM, HMOH 1.0 mM, NH_4OH 16 mM, DTPA 0.1 mM) pH 9.0. CE conditions: injection 20 mbar for 5 s, capillary length 64.5 cm, applied voltage -30kV, temperature 25°C.

Although the sulfur balance cannot be fully closed, as there are species that we do not or cannot measure during these experiments, it can be seen that the concentrations of all the species vary with time (Figure 3.2). This is related to the complex nature of the reactions between the various sulfur-containing anions. Nevertheless, the system appeared to begin to reach an equilibrium around 2 hours, with thiosulfate, sulfate and sulfite reaching a plateau (Figure 3.3).

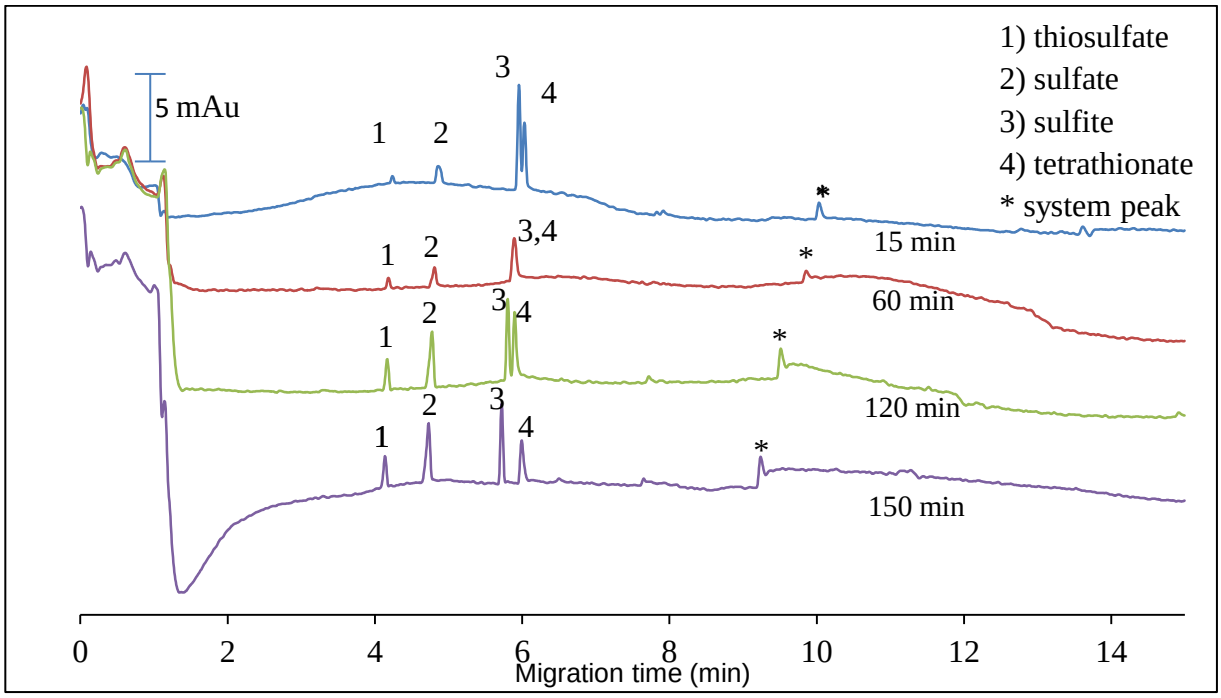

Figure. 3.2. Mixture of $S_4O_6^{2-}$ 0.66 mM, SO_3^{2-} 0.40 mM, BGE: PMA 2.0 mM, HMOH 0.8 mM, NH_4OH pH 9.0, DTPA 0.1 mM. CE conditions: capillary length 64.5 cm, injection 100 mbar. s., applied voltage -30 kV, temperature 25 °C. Spectra acquired at 214 nm with reference at 360 nm.

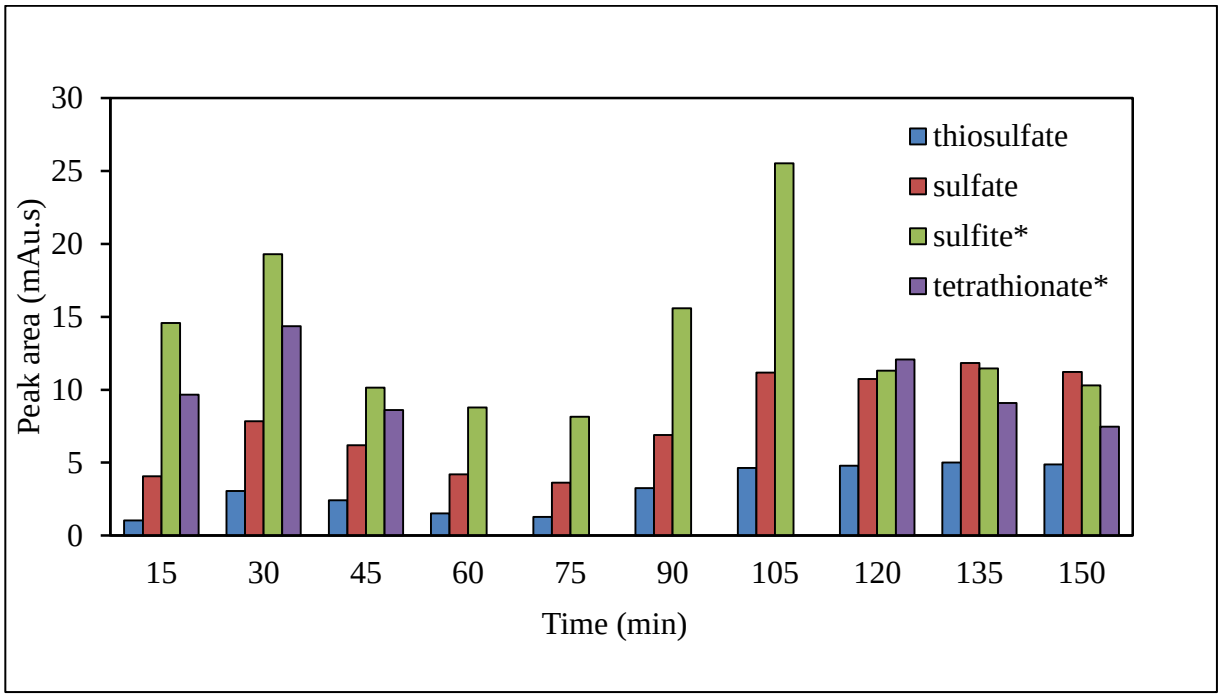

Figure 3.3. Changing of peak area (PA) with injection time (15 min) to (150 min) over 10 runs (Figure 3.2) with the same sample (sulfite, tetrathionate), and no replenishment for the BGE. * starting material.

During the rearrangement reaction between tetrathionate and sulfite, sulfur, sulfide, or other intermediates which may be formed depending on the particular conditions as pH and the relative nucleophilicity of sulfur oxyanions which are affected by these mechanisms.[5,15,18]

Tetrathionate initiated decomposition in alkaline media via scission of the inner S-S bond yields thiosulfate and $S_2O_3OH^-$. The formation of the adduct, $S_4O_6OH^{3-}$, is probably followed by heterolytic inner S-S bond cleavage resulting in the nucleophilic displacement of thiosulfate by hydroxide ion (Eq. 3.16):

$$S_4O_6^{2-} + OH^- \longrightarrow S_2O_3^{2-} + S_2O_3OH^- \qquad (3.28)$$

The intermediate product $HOS_2O_3^-$ can decompose into thiosulfate and sulfite:

$$2S_2O_3OH^- + 4OH^- \longrightarrow S_2O_3^{2-} + 2SO_3^{2-} + 3H_2O \quad (3.29)$$

Decomposition of $HOS_2O_3^-$, according to the report of Varga et al. (2007), is not elementary and probably proceeds via the following consecutive processes where the formation of an intermediate disulfite, $S_2O_5^{2-}$ occurs:[15]

$$2S_2O_3OH^- \longrightarrow S_2O_3^{2-} + S_2O_5^{2-} + 2H^+ \quad (3.30)$$

$$S_2O_5^{2-} + H_2O \longrightarrow 2SO_3^{2-} + 2H^+ \quad (3.31)$$

$S_2O_3OH^-$ can also react with tetrathionate and forms sulfate and pentathionate. The amount of pentathionate and sulfate formed increases with the increasing initial tetrathionate concentration:

$$S_4O_6^{2-} + S_2O_3OH^- \longrightarrow S_5O_6^{2-} + SO_4^{2-} + H^+ \quad (3.32)$$

The well-known reversible rearrangement of tetrathionate occurs in the presence of thiosulfate as a catalyst, providing a sufficiently low level of pentathionate (not a detectable amount), and sulfite as shows in (Eq. 3.6).[5,7,15]

The sulfitolysis step is the following reaction as sulfite and tetrathionate are in the mixture. Trithionate is only produced from this step and may as well appear as a final product with increasing sulfite concentration from alkaline decomposition of tetrathionate (Eq. 3.4).[7,15,6,18]

Sulfite experiences hydrolysis reaction as well:[5]

$$SO_3^{2-} + H_2O \longrightarrow HSO_3^- + OH^- \quad (3.33)$$

In alkaline solutions, pentathionate decomposes very quickly to thiosulfate and $S_3O_3OH^-$ where it is attacked by hydroxide ion at the γ-sulfur atom.[15,19] The $S_3O_3OH^-$ intermediate can undergo further hydrolysis to form other intermediates such as $S_2O_3OH^-$, and $S(OH)_2$:

$$S_5O_6^{2-} + OH^- \longrightarrow S_2O_3^{2-} + S_3O_3OH^- \quad (3.34)$$

$$S_5O_6^{2-} + 3OH^- \longrightarrow 2.5S_2O_3^{2-} + 1.5H_2O \quad (3.35)$$

$$S_3O_3OH^- + OH^- \longrightarrow S_2O_3^{2-} + S(OH)_2 \quad (3.36)$$

$$S_4O_6^{2-} + S_3O_3OH^- \longrightarrow S_5O_6^{2-} + S_2O_3OH^- \quad (3.37)$$

Sulfoxylic acid $S(OH)_2$, in Eq. 3.36, decomposes very fast to produce sulfite and soluble sulfur HS(OH) as it is a short- lived intermediate under alkaline conditions:

$$2S(OH)_2 + 2OH^- \longrightarrow SO_3^{2-} + HS(OH) + 2H_2O \quad (3.38)$$

Soluble sulfur in the form of HS(OH) reacts with sulfite to produce thiosulfate, while it decomposes to form sulfur precipitation in the lack of sulfite:[5,7,15]

$$SO_3^{2-} + HS(OH) \longrightarrow S_2O_3^{2-} + H_2O \quad (3.39)$$

$$HS(OH) \longrightarrow S + H_2O \quad (3.40)$$

At the same time, pentathionate $S_5O_6^{2-}$ ions experience a rearrangement reaction in the presence of a high concentration of $S_2O_3^{2-}$ to give $S_4O_6^{2-}$ and hexathionate ($S_6O_6^{2-}$). Hexathionate also decomposes to pentathionate and sulfur elements:[5]

$$2S_5O_6^{2-} + 4S_2O_3^{2-} \longrightarrow 3S_4O_6^{2-} + S_6O_6^{2-} \quad (3.41)$$

$$S_6O_6^{2-} \longrightarrow S_5O_6^{2-} + S \qquad (3.42)$$

Sulfur element precipitation affects capillary surface chemistry that impacts the migration behaviour of sulfur species, especially tetrathionate, as it has a greater mass and size as illustrated in Table 3.1.

The reactants, the end products, and the solvent all play important roles in the reaction of sulfite and tetrathionate in alkaline media. These reactions can explain the amount of individual sulfur species as they increase and decrease, even to the point of disappearance, during the course of this study Figure (3.2, 3.3).[5,7,11,17,19]

Table 3.1. Peak area (PA, mAU.s), migration time (t_m, minute), average, standard deviation (SD), and relative standard deviation (% RSD) for replicate analysis (n=10) for the same mixture ($S_4O_6^{2-}$ and SO_3^{2-}) and no BGE replenishment, Figure (3.2).

Analyte	PA_1 (t_{m1})	PA_2 (t_{m2})	PA_3 (t_{m3})	PA_4 (t_{m4})	PA_5 (t_{m5})	PA_6 (t_{m6})	PA_7 (t_{m7})	PA_8 (t_{m8})	PA_9 (t_{m9})	PA_{10} (t_{m10})	Mean PA, (t_m)	SD PA, (t_m)	%RSD PA, (t_m)
$S_2O_3^{2-}$	1.03 (4.24)	3.06 (4.19)	2.43 (4.25)	1.51 (4.18)	1.27 (4.28)	3.26 (4.25)	4.64 (4.18)	4.80 (4.17)	5.00 (4.15)	4.87 (4.14)	3.187 (4.20)	1.504 (0.05)	47.18 (1.08)
SO_4^{2-}	4.06 (4.80)	7.85 (4.81)	6.20 (4.90)	4.19 (4.81)	3.63 (4.93)	6.89 (4.89)	11.18 (4.80)	10.73 (4.77)	11.83 (4.75)	11.21 (4.73)	7.779 (4.82)	3.094 (0.06)	39.77 (1.30)
SO_3^{2-}	14.58 (5.97)	19.30 (5.84)	10.14 (5.98)	8.78* (5.89)	8.15* (6.08)	15.58* (6.00)	25.52* (5.86)	11.31 (5.80)	11.47 (5.76)	10.29 (5.72)	13.512 (5.89)	5.147 (0.11)	38.09 (1.81)
$S_4O_6^{2-}$	9.66 (6.03)	14.36 (5.90)	8.61 (6.02)					12.08 (5.90)	9.08 (5.94)	7.46 (5.99)	6.125 (5.96)	5.315 (0.05)	86.78 (0.90)

* SO_3^{2-} and $S_4O_6^{2-}$ are comigrating in these experiments.

Bisulfide was successfully identified using two different standards, Na_2S, and $HNaS.xH_2O$, under basic conditions (Figure 3.4 (a, b)). Bisulfide in the mixture of thiosulfate, chloride, sulfate, tetrathionate, and sulfite can negatively affect analysis in various ways. For example, bisulfide reacts with sulfite to produce thiosulfate, and this was observed with an increase in the peak area of $S_2O_3^{2-}$ from 13.34 to 43.82 mAU.s (Eq. 3.16). Meanwhile, thiosulfate can be hydrolyzed to sulfate and bisulfide, which maintains the presence of HS^- in the mixture:

$$S_2O_3^{2-} + H_2O \longrightarrow SO_4^{2-} + HS^- + 2H^+ \quad (3.43)$$

Sulfuric acid dissociates to produce sulfate and protons:

$$H_2SO_4 \longrightarrow SO_4^{2-} + 2H^+ \quad (3.44)$$

Bisulfide also decomposes to elemental sulfur (Eq. 3.17) then the sulfur can react with sulfite to produce thiosulfate or tetrathionate (Eq. 3.18, 3.19). Elemental sulfur also reacts with sulfuric acid and released sulfur dioxide, which also makes full accounting in the sulfur balance more challenging, and explains the reduction in sulfate with time (Table 3.2):

$$2H_2SO_4 + S \longrightarrow 3SO_2 + 2H_2O \quad (3.45)$$

However, the participation of sulfite in these reactions caused a decreased in its amount, and this led to fusion with tetrathionate as shown in Figure 3.4 (d).

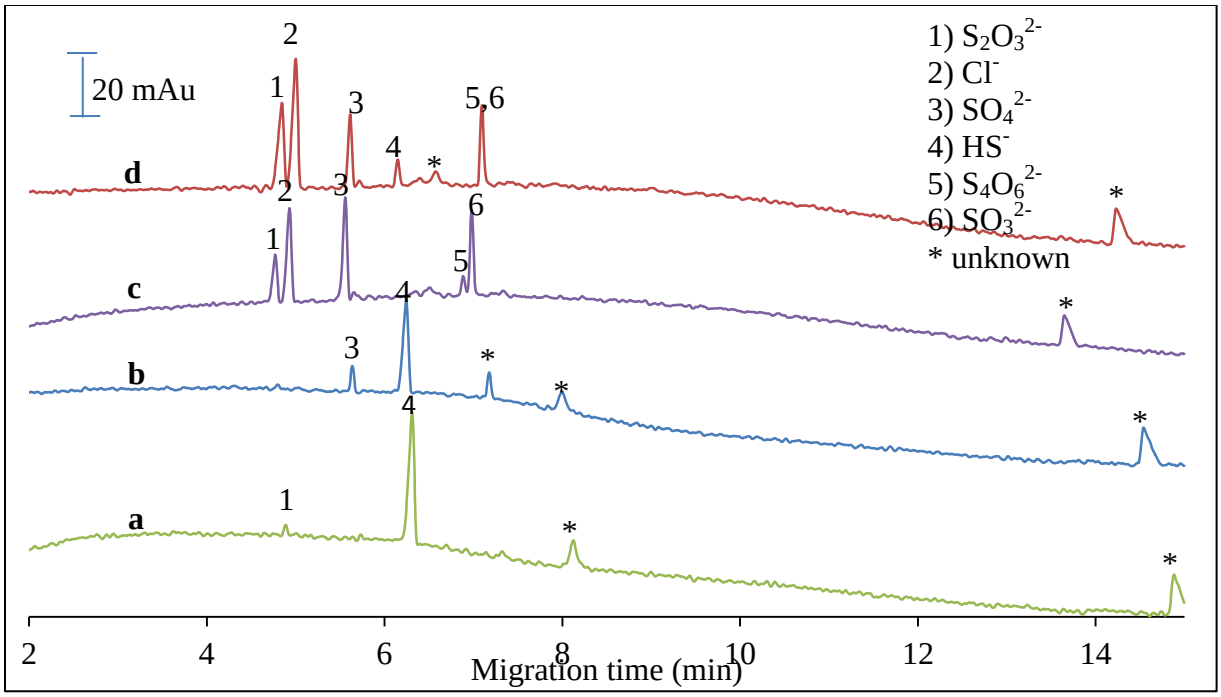

Figure 3.4. Standards: a) HS^- 3.57 mM, b) S^{2-} 2.56 mM, c) Mixture of ($S_2O_3^{2-}$ 0.20 mM, Cl^- 0.86 mM, SO_4^{2-} 0.35 mM, SO_3^{2-} 0.40 mM, and $S_4O_6^{2-}$ 0.17 mM, d) Mixture (c) with S^{2-} 0.64 mM. BGE (PMA 6.0 mM, HMOH 1.0 mM, DTPA 0.1 mM, NH_4OH pH 9.0. CE conditions: capillary length 64.5 cm, injection 20 mbar for 5 s., applied voltage -30 kV, temperature 25 °C. Spectra acquired at 214 nm with reference at 360 nm.

Table 3.2. Peak area (PA, mAu.s) and migration time (t_m, minute) for mixture of $S_2O_3^{2-}$, Cl^-, SO_4^{2-}, S^{2-}, $S_4O_6^{2-}$, SO_3^{2-}, and the same mixture with added sulfide anion, and sulfide alone from Na_2S, Figure (3.4)

Analyte	$S_2O_3^{2-}$		Cl^-		SO_4^{2-}		S^{2-}		SO_3^{2-}		$S_4O_6^{2-}$	
	PA	t_m	PA	t_m	PA	t_m	PA	t_m	PA	t_m	PA	t_m
Without sulfide	13.34	4.77	27.45	4.93	27.73	5.56	ND	ND	4.68	6.88	18.50	6.98
With sulfide	43.82	4.85	30.95	5.00	16.57	5.61	6.64	6.15	18.14*	7.10*	18.14*	7.10*
Sulfide alone	ND	ND	ND	ND	ND	ND	30.39	6.24	ND	ND	ND	ND

ND- not detected

* SO_3^{2-} and $S_4O_6^{2-}$ are combining after sulfide addition

3.6 Conclusions

Sulfur containing anions are highly reactive toward each other. From the information gathered in the CE experiments, and reactions previously proposed, we have proposed a few general reaction pathways in the reactivity of thiosulfate, sulfate, hydrogen sulfide anion, tetrathionate, and sulfite. Sulfite and tetrathionate reacted to each other, producing various sulfur-containing species over time depending on the particular conditions as pH and the relative nucleophilicity of sulfur oxyanions. Even though we could not measure all the species that were present during the experiment, some of sulfur species were identified, such as thiosulfate, sulfate, tetrathionate, and sulfite according to their migration time. There were many behaviours observed for some of the sulfur species in the system including concentrations that decreased, increased and those that did not change within analysis time. The bisulfide also reacted in different reactions in mixture of thiosulfate, sulfate, tetrathionate, and sulfite. Hence, all the component, including the reactants, the end products, and the solvent play important roles in the reactions between sulfur species in alkaline media. These pathways will be important in developing methods to control sulfur species in offshore oil and gas reservoirs

3.7 References

(1) Druschel, G. K.; Hamers, R. J.; Banfield, J. F. *Geochim. Cosmochim. Acta* **2003**, *67* (23), 4457–4469.

(2) Kuyucak, N.; Yaschyshyn, D. *Mining and the Environment IV Conference* **2007**, 705.

(3) Xu, Y.; Schoonen, M. A. A.; Nordstrom, D. K.; Cunningham, K. M.; Ball, J. W. *J. Volcanol. Geotherm. Res.* **2000**, *97* (1–4), 407–423.

(4) Yilmaz, Ü. T.; Somer, G. *Anal. Chim. Acta* **2007**, *603* (1), 30–35.

(5) Zhang, H.; Jeffrey, M. I. *Inorg. Chem.* **2010**, *49* (22), 10273–10282.

(6) Pan, C.; Wang, W.; Horváth, A. K.; Xie, J.; Lu, Y.; Wang, Z.; Ji, C.; Gao, Q. *Inorg. Chem.* **2011**, *50* (19), 9670–9677.

(7) Lu, Y.; Gao, Q.; Xu, L.; Zhao, Y.; Epstein, I. R. *Inorg. Chem.* **2010**, *49* (13), 6026–6034.

(8) Harstad, R. K.; Johnson, A. C.; Weisenberger, M. M.; Bowser, M. T. *Anal. Chem.* **2016**, *88* (1), 299–319.

(9) Petre, C. F.; Larachi, F. *J. Sep. Sci.* **2006**, *29*, 144–152.

(10) Hughes, M. N.; Centelles, M. N.; Moore, K. P. *Free Radic. Biol. Med.* **2009**, *47* (10), 1346–1353.

(11) Laine, P.; Matilainen, R. *Anal. Bioanal. Chem.* **2005**, *382* (7), 1601–1609.

(12) O'Reilly, J. W.; Dicinoski, G. W.; Shaw, M. J.; Haddad, P. R. *Anal. Chim. Acta* **2001**, *432* (2), 165–192.

(13) Tobergte, D. R.; Curtis, S. *J. Chem. Inf. Model.* **2013**, *53* (9), 1689–1699.

(14) Zopfi, J. *Geological Society of America* **2004**, 379, 97–116.

(15) Varga, D.; Horváth, A. K. *Inorg. Chem.* **2007**, *46* (18), 7654–7661.

(16) Miranda-Trevino, J. C.; Pappoe, M.; Hawboldt, K.; Bottaro, C. *Crit. Rev. Environ. Sci. Technol.* **2013**, *43*, 2013–2070.

(17) Vongporm, Y. Master thesis, *Memorial University ofNewfoundland*, **2008**.

(18) Ericka L. Barrett and Marta A. Clark. *Microbiol. Rev.* **1987**, *51* (2), 192–205.

(19) Voslar, M.; Matejka, P.; Schreiber, I. *Inorg. Chem.* **2006**, *45* (7), 2824–2834.

(20) Foss, O. *Acta Chem. Scand*. **1958**, 12 (5), 959–966.

(21) Ahern, N.; Dreisinger, D.; Weert, G. VAN. *Can. Metall. Q.* **2006**, *45* (2), 135–144.

Chapter 4. Oxidation- Reduction for Sulfur Oxygen Species

4.1 Introduction

The sulfur compounds under study in this thesis are particularly challenging because of their labile nature and complex redox chemistry. It would be expected that under ideal and controlled temperatures and pH conditions that species interconversion would be minimized. Given that CZE is a electromigration technique, the system can also be viewed as an electrochemical cell in which electrochemical reactions will occur. This adds an extra measure of complexity to an already challenging chemical system. Consequently, a basic understanding of the principles associated with the coupling of electrochemistry, and electromigration phenomena is critical for the optimization capillary electrophoresis system.[1,2]

In a typical CZE (Figure 4.1), the migration of the ions is initiated when a potential is applied to direct current (DC) electrodes inserted into reservoirs containing a background electrolyte (BGE). An electric field in BGE is facilitated by both electron transfer to and from the electrode (Faradaic current) and ionic current (Ohmic). Redox reactions occur at the electrode depending on its polarity and electrolyte pH. The reactions are driven by current and electroosmotic flow in the CE system. Of the potential electrochemical reactions that can occur at the electrodes during an electrophoretic run, water electrolysis dominantes and it is partially through this process that the charge balance is maintained in the system.[3,4] Such electrolysis (Eq. 4.1, 4.2) is most efficient under alkaline conditions, which are also the conditions that give the highest EOF.[1,3,4] At

the anode, oxygen is produced through the oxidation of hydroxyl ions from the autoionization of water (Eq. 4.1). Decreasing hydroxyl ion concentration leads to a decrease of the pH of the solutions, which affects the ionization of the chromophoric probe (PMA). At the cathode, on the other hand, there is an accumulation of positive charges that are neutralized by hydroxyl ions, resulting in an increase in the solution pH (Eq. 4.2):[1]

Anode: $4OH^- \longrightarrow 4e^- + O_2 + 2H_2O$ (4.1)

Cathode: $2H_2O + 2e^- \longrightarrow H_2 + 2OH^-$ (4.2)

The gas produced in electrolysis can have negative consequences for CE separations. The gases bubbles can dislodge from the electrode surface and flow from the reservoir into the capillary, causing blockage or oxidation of other species. The presence of the gases either adsorbed or in the capillary can increase interelectrode resistance, resulting in a current drop for potentiostatic operation.[1] Electroosmotic flow, shapes of peaks in the electropherograms, and the pH of the background electrolyte can all be negatively impacted by such dissociation reactions (Eq. 4.1, 4.2). However, the most important effects are on the pH of the system and the potential for electrochemical reactions with the analytes, noting that thiosalts are most stable under slightly alkaline conditions, and that the stability of the analytes is critical for reliability of any analytical method.

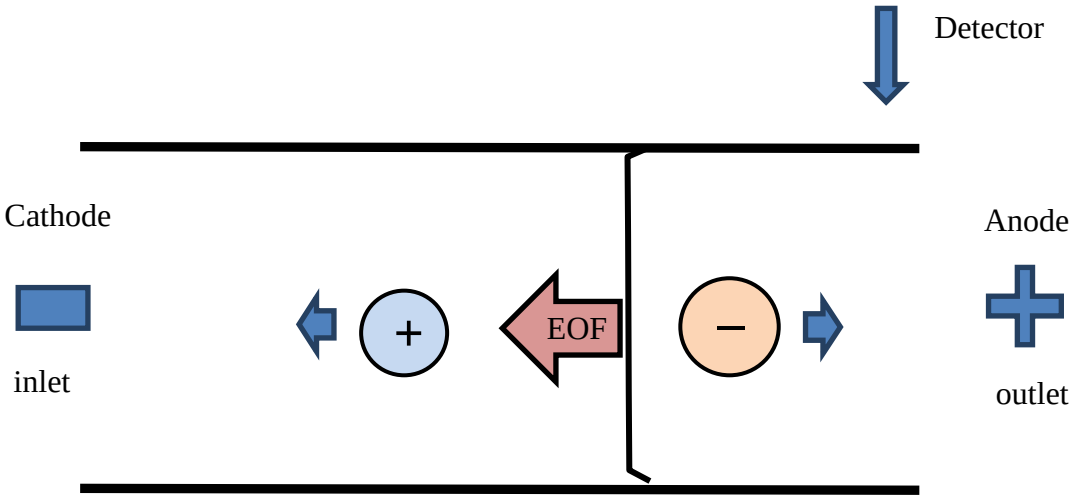

Figure 4.1. Schematic of CE process.

Acid-base equilibria and buffer properties, including pH in the electrode reservoirs and capillary, are strongly affected by these electrochemical reactions and redistribution of ions between the anode and cathode electrolytes lead to a problem in CE.[1,3,4]

In addition to the water electrolysis reactions, many reactions can occur between additives or analytes, particularly for the sulfur-containing anions under study. The nature and extent of these reactions depend on the conditions of the experiment. For example, cathodic reactions can be simple electrochemical reductions, as with tetrathionate and sulfate, which are easily reduced according to reactions 4.3 and 4.4, noting the low standard reduction potentials of the half reactions:[5,6,7]

$$S_4O_6^{2-} + 2e^- \rightleftharpoons 2S_2O_3^{2-} \qquad E^o = +\,0.17\ V \qquad (4.3)$$

$$SO_4^{2-} + 2H^+ + 2e^- \rightleftharpoons SO_3^{2-} + H_2O \qquad E^o = +\,0.20\ V \qquad (4.4)$$

The generation of oxygen at the anode can lead to a range of oxidation reactions among thiosalts. According to Voslar et al. (2006), the oxidation of tetrathionate in alkaline

solution leads to formation of thiosulfate, sulfate, and sulfite.[8] The thiosulfate can then be oxidized to the reactive peroxothiosulfate intermediate $HOS_2O_3^-$ which may undergo further interactions as described in Scheme 4.1:[8]

$$S_4O_6^{2-} + 4OH^- + O_2 \longrightarrow S_2O_3^{2-} + SO_3^{2-} + SO_4^{2-} + 2H_2O \quad \text{(R1)}$$

$$S_4O_6^{2-} + SO_3^{2-} \longrightarrow S_3O_6^{2-} + S_2O_3^{2-} \quad \text{(R2)}$$

$$2S_2O_3^{2-} + H_2O + O_2 \longrightarrow 2HOS_2O_3^- + 2OH^- \quad \text{(R3)}$$

$$2HOS_2O_3^- + 2H_2O + O_2 \longrightarrow 4HSO_3^- + 2H^+ \quad \text{(R4)}$$

$$HOS_2O_3^- + H^+ + S_2O_3^{2-} \longrightarrow S_4O_6^{2-} + H_2O \quad \text{(R5)}$$

$$H_2O + O_2 + SO_3^{2-} \longrightarrow 2SO_4^{2-} + H_2O \quad \text{(R6)}$$

$$H_2O + O_2 + 2HSO_3^- \longrightarrow 2SO_4^{2-} + H_2O + 2H^+ \quad \text{(R7)}$$

$$H_2O \longrightarrow OH^- + H^+ \quad \text{(R8)}$$

$$HSO_3^- \longrightarrow SO_3^{2-} + H^+ \quad \text{(R9)}$$

Scheme 4.1. Mechanism for tetrathionate oxidation reactions with subsequent oxidation of other thiosalts.

In this chapter, an attempt was made to study redox reactions for sulfur species due to electron transfer and oxygen generation in alkaline solution during CE operation over a range of time.

4.2 Experimental Method

All chemicals and reagents were of highest purity and used without further purification. Oxidation-reduction reactions for sulfur-oxygen species were examined in a simple aqueous solution with various components present (sodium sulfate anhydrous, sodium thiosulfate, potassium tetrathionate, and sodium chloride all purchased from Sigma-Aldrich). The test was completed in a BGE of PMA at 2.0 mM, HMOH at 0.8 mM, and the pH was adjusted to 9.0 with ammonium hydroxide. The test solutions were made up to the required concentrations using deoxygenated LC water (Fisher Chemical, UK) containing DTPA (0.1 mM) to bind reactive metal impurities such as iron(III), and copper(II). Stock solutions of 1000 mg/L of sulfur oxyanions salts and BGE were also degassed and filtered with a 0.22 µm nylon syringe filter (Canadian Life Science, ON). All solutions were sealed in amber tubes and kept at 4 °C, except during analysis to minimize undesirable reactions. Test solutions were containing 0.20 mM $S_2O_3^{2-}$, 0.86 mM Cl^-, 0.35 mM SO_4^{2-}, 0.40 mM SO_3^{2-}, 0.17 mM $S_4O_6^{2-}$ where prepared fresh daily. The experiments were done by using Agilent 7100 ^{3D} CE System (Agilent Technologies Canada Inc., Mississauga, ON) using an indirect detection method based on measurements at 360 nm with a reference wavelength of 214 nm. The test was run for 75 minutes with the same vial of the samples and without replenishment the BGE.

This study shows the oxidation- reduction for sulfur oxygen species inside the CE over a period of time. This involved studying the reaction over short periods of time before any significant changes in concentration of the reactants occurred (45 mins). The reactivity of each species was identified by comparing peak area during different injection times.

4.3 Results and Discussion

In an alkaline solution, the transient formation of thiosulfate as well as the formation of a significant amount of trithionate, which was attributed to reactions R1 and R2, was clearly visible over 5 runs. A second oxidation occurred for thiosulfate and sulfite after tetrathionate oxidation. Tetrathionate and sulfate were the production of the secondary oxidation. Figure 4.2 displays the relationship between the reactant mixture and the production of oxygen over time (15 min-75 min) according to the series of reactions in Scheme 4.1.

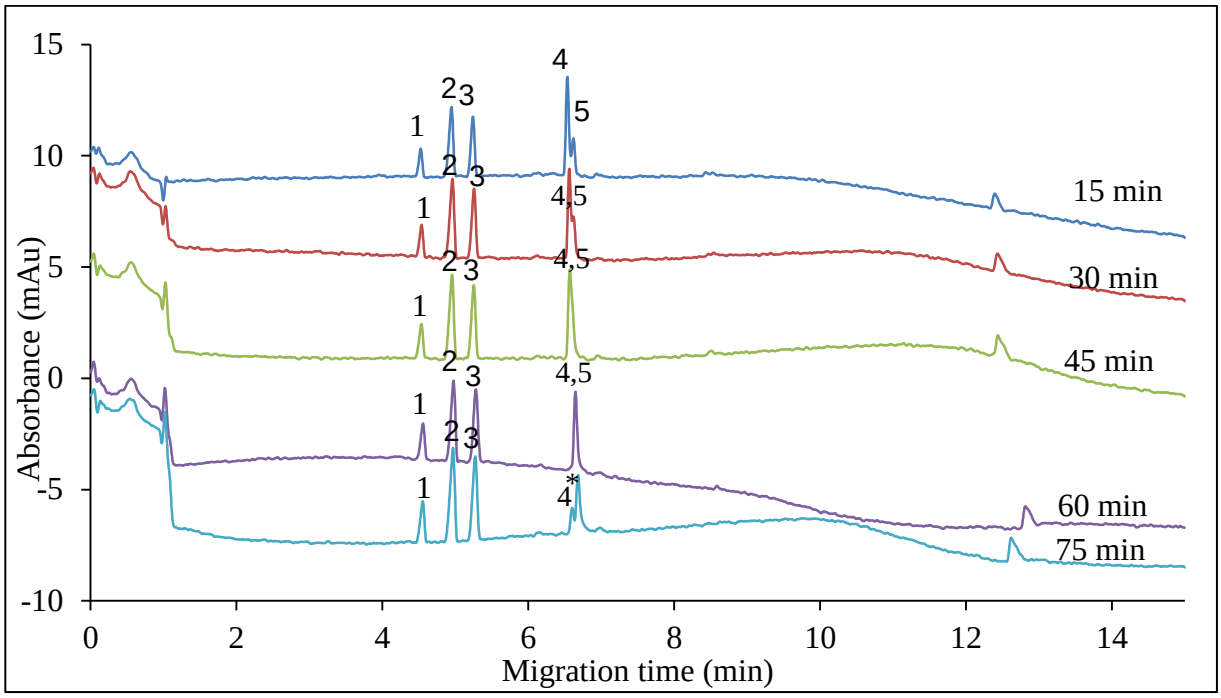

Figure 4.2. Mixture of 1) $S_2O_3^{2-}$ 0.20 mM, 2) Cl^- 0.86 mM, 3) SO_4^{2-} 0.35 mM, 4) SO_3^{2} 0.40 mM, 5) $S_4O_6^{2-}$ 0.17 mM. BGE (PMA 2.0 mM, HMOH 0.8 mM, DTPA 0.1 mM, NH_4OH pH 9.0). CE conditions: capillary length 64.5 cm, injection 20 mbar for 5 s, applied voltage -30 kV, temperature 25 °C. Spectra acquired at 214 nm with reference at 360 nm.

The impact of the separation conditions on the analyte stability was assessed by plotting analyte peak area (Table 4.1) against the time of injection (Figure 4.3). All analytes showed more stable results using replenished BGE, with very slight trends toward consumption leading to reduced concentrations for sulfate and tetrathionate, or formation for thiosulfate and sulfite. These changes can be attributed to reactions occurring in the sample vials, and are not problematic if samples are used quickly after warming to the analysis temperature. Conversely, the conditions generated within the capillary when the run buffer is not replenished have a substantial effect. Thiosulfate formation is accelerated and sulfate seems to be forming rather than being slowly consumed.

However, the initial concentration of sulfate is also depleted relative to the replenished system, which may explain the sharp increases in tetrathionate and sulfite in the second injection, where sulfate has likely undergone a transformation that results in their formation. At the same time, tetrathionate and sulfite are reacting to form thiosulfate and reform sulfate, and this is illustrated in their decreasing concentrations at later injection times. These profound changes in the concentrations of the various species, are strong evidence for changes in redox conditions due to hysteresis when the BGE in the CE system is not replenished.[1,3,4]

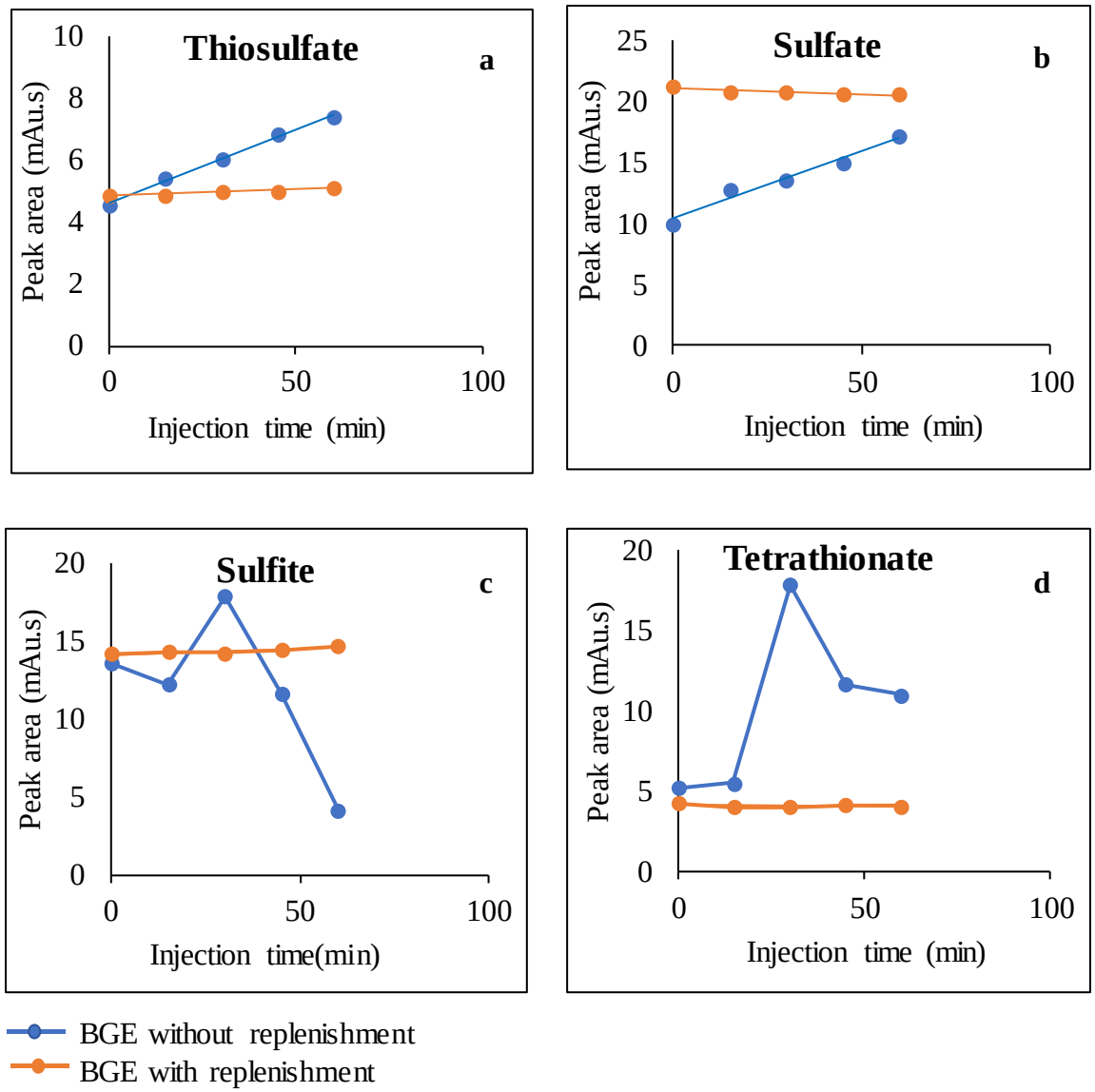

Figure 4.3. (a, b, c, d) Comparison between non-replenishment and replenishment BGE for the mixture in Figure 4.1 and Figure 4.3.

Table 4.1. Migration time (tm) and peak area (PA) for replicate analysis (5 runs) of mixture of $S_2O_3^{2-}$, Cl^-, SO_4^{2-}, SO_3^{2-}, $S_4O_6^{2-}$ with using non-replenishment BGE (PMA 2.0 mM, HMOH 0.8 mM, DTPA 0.1 mM, NH_4OH pH 9.0) Figure 4.2.

Run	t_m $S_2O_3^{2-}$	PA $S_2O_3^{2-}$	t_m Cl^-	PA Cl^-	t_m SO_4^{2-}	PA SO_4^{2-}	t_m SO_3^{2-}	PA SO_3^{2-}	t_m $S_4O_6^{2-}$	PA $S_4O_6^{2}$-
r_1	4.52	4.58	4.95	12.90	5.24	9.97	6.53	13.56	6.62	5.19
r_2	4.54	5.42	4.96	14.85	5.26	12.78	6.56	12.21	6.62	5.48
r_3	4.53	6.02	4.96	16.58	5.25	13.49	6.57	17.86	6.57	17.86
r_4	4.56	6.82	4.98	15.68	5.28	14.96	6.65	11.64	6.65	11.64
r_5	4.55	7.40	4.97	18.80	5.27	17.15	6.60	4.15	6.68	10.95
Mean	4.54	6.05	4.96	15.76	5.26	13.67	6.58	11.88	6.63	10.23
SD	0.01	1.12	0.01	2.18	0.02	2.66	0.04	4.96	0.04	5.21
%RSD	0.3	18.5	0.2	13.8	0.3	19.4	0.7	41.8	0.62	51.0

For the analysis of high oxidation of sulfur containing anions using CE, there is a need to minimize gas generation during CE operation. By refilling the reservoir solutions (BGE) after every single run and flushing the capillary, the gas generation was minimized and its effects are illustrated in Figure 4.4. [1,3]

Table 4.2 displays the successes of reducing the generation of gases as the peak areas for the mixture of $S_2O_3^{2-}$, Cl^-, SO_4^{2-}, SO_3^{2-}, $S_4O_6^{2-}$ were consistent in replicate runs. Additionally, this improvement in stability was illustrated by plotting both non-replenishment and replenishment BGE based on electropherograms shown in Figure 4.2.

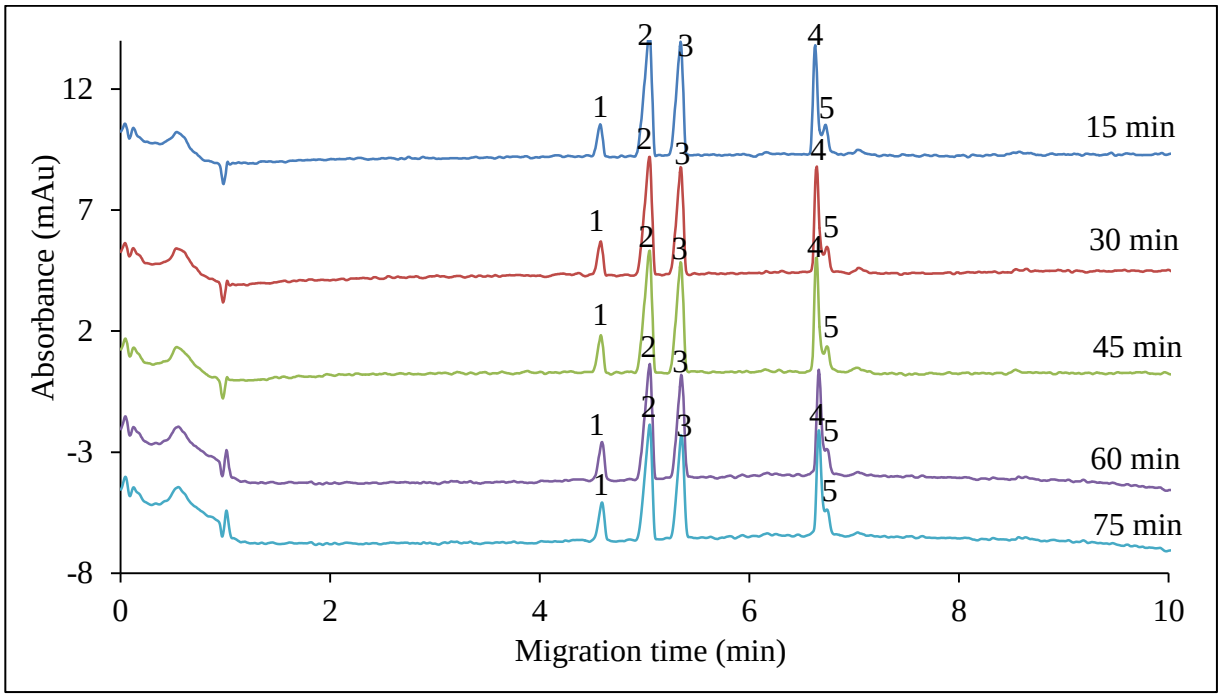

Figure 4.4. Mixture of 1) $S_2O_3^{2-}$ 0.20 mM, 2) Cl^- 0.86 mM, 3) SO_4^{2-} 0.35 mM, 4) SO_3^{2-} 0.40 mM, 5) $S_4O_6^{2-}$ 0.17 mM. BGE (PMA 2.0 mM, HMOH 0.8 mM, DTPA 0.1 mM, NH_4OH pH 9.0). CE conditions: capillary length 64.5 cm, injection 20 mbar for 5 s, applied voltage -30 kV, temperature 25 °C. Spectra acquired at 214 nm with reference at 360 nm.

Table 4.2. Migration time (tm) and peak area (PA) for replicate analysis (5 runs) of mixture of $S_2O_3^{2-}$, Cl^-, SO_4^{2-}, SO_3^{2-}, $S_4O_6^{2-}$. with using replenishment BGE (PMA 2.0 mM, HMOH 0.8 mM, DTPA 0.1 mM, NH_4OH pH 9.0) Figure 4.4.

Run	t_m $S_2O_3^{2-}$	PA $S_2O_3^{2-}$	t_m Cl^-	PA Cl^-	t_m SO_4^{2-}	PA SO_4^{2-}	t_m SO_3^{2-}	PA SO_3^{2-}	t_m $S_4O_6^{2-}$	PA $S_4O_6^{2-}$
r_1	4.58	4.88	5.05	26.57	5.34	21.33	6.63	14.13	6.73	4.21
r_2	4.58	4.88	5.05	25.28	5.35	20.78	6.64	14.29	6.74	4.02
r_3	4.58	4.98	5.05	25.30	5.35	20.79	6.64	14.22	6.74	4.01
r_4	4.59	4.99	5.05	25.34	5.35	20.64	6.66	14.41	6.73	4.11
r_5	4.59	5.14	5.05	25.65	5.35	20.65	6.66	14.67	6.71	4.07
Mean	4.584	4.972	5.046	25.627	5.347	20.839	6.646	14.343	6.729	4.085
SD	0.006	0.109	0.001	0.548	0.003	0.282	0.014	0.211	0.014	0.082
%RSD	0.133	2.195	0.018	2.140	0.052	1.354	0.205	1.470	0.208	2.012

4.5 Conclusions

Electrolyte chemistry, shapes of electropherograms, and pH of background electrolyte are affected by species dissociation and buffer system reactions on the electrode in typical capillary electrophoresis. Reduction and oxidation (redox) reaction occurrence depend on the pH of the solution and electrode polarity. Water electrolysis is the most dominant of the electrode reactions. Water electrolysis is often associated with the generation of hydrogen and oxygen gases. These gases can block the connection between a solution and electrode or be entrained into the capillary. Oxygen gas is also a strong oxidizing agent, leading to oxidization of the sulfur-oxygen species and producing a mix of products.

Redox reactions can be observed after the first three separation runs and impacts the performance of the entire system. Reproducible and stable currents are the keys for successful separations. Gas generation, along with the resulting effects, can be minimized by refilling the reservoir solutions (BGE) after every single run and flushing the capillary. Overall, the coupling between electrochemistry and electromigration phenomena have significant effect on analysis and optimization of capillary zone electrophoresis.

4.6 References

(1) Persat, A.; Suss, M. E.; Santiago, J. G. *Lab Chip* **2009**, *9* (17), 2454–2469.

(2) Kirby, B. J.; Hasselbrink, E. F. *Electrophoresis* **2004**, *25* (2), 187–202.

(3) Revermann, T.; Götz, S.; Künnemeyer, J.; Karst, U. *Analyst* **2008**, *133* (2), 167–174.

(4) Bello, M. S. *J. Chromatogr. A* **1996**, *744* (1–2), 81–91.

(5) Ericka L. Barrett and Marta A. Clark. *Microbiol. Rev.* **1987**, *51* (2), 192–205.

(6) Kaprálek, F. *J. Gen. Microbiol.* **1972**, *71* (1), 133–139.

(7) Vogel, A. **1979,** Vogel's Qualitative Inorganic Analysis (5th edition). New York, U.S.A: Long Man limited.

(8) Voslar, M.; Matejka, P.; Schreiber, I. *Inorg. Chem.* **2006**, *45* (7), 2824–2834.

Chapter 5. Conclusions and Future Work

5.1 General Conclusions

It is accepted that the chemistry of sulfur and its contribution to reservoir souring is complex, however this does not mean that the mechanisms are fully understood or verified. [1-5] Understanding the chemistry of the reservoir souring process so that the reductive or oxidative processes can be reduced requires methods to quantify all the key sulfur species. CE has been used for the analysis of inorganic sulfur-containing anions in very complex matrices due to its high separation efficiency and speed, low cost of consumables, and high tolerance to sample matrices with high ionic strength.[2,6,7,8,9,13-15] The goals of the work presented in this thesis were to simplify and improve existing analytical methods in terms of sensitivity, selectivity, reproducibility and robustness, as well as to make modifications to the methods so that they can be used with reservoir fluids and produced water. The results of this research demonstrate that by using two CZE methods, one with direct detection and the other with indirect detection, most of the sulfur anions can be analyzed even in the presence of chloride, which is a common challenge for environmental anion analysis.

A number of factors were considered in improving the existing CE methods. For example, the concentration and nature of the chromophoric probe (PMA), the concentration of the EOF modifiers (HMOH), the nature and pH of the pH-control system were optimized, as well as capillary length, and separation temperature. For indirect detection, pyromellitic acid (PMA= 6.0 mM) was selected as the chromophoric probe to

detect non-absorbing anions because it is non-oxidizing, has high molar absorptivity (high sensitivity), and is a good mobility match for thiosalts.[6,20] Hexamethonium hydroxide (HMOH =1.0 mM) was added to modify the capillary surface chemistry and suppress EOF, resulting in methods with a shorter time of analysis and better peak resolution.[8,18,14,19] Weakly basic conditions are favoured (pH 9.0) since thiosulfate is decomposed in acidic media. Furthermore, ionization of weakly acidic sulfur species (sulfite and sulfide) and PMA are efficiently ionized at this pH.[1,3,9,23,24]

Indirect CZE was able to accommodate the species of interest with detection at 360 nm and a reference wavelength of 214 nm, but there was a challenge in separating chloride from thiosulfate in briny waters where chloride is found in abundance. The direct method was applied to solve this problem, where thiosulfate absorbs UV, in contrast to chloride which is essentially invisible. The BGE for direct detection was optimized through the EOF modifier (HMOH) concentration and buffer system (pH 9.0), that was adjusted with formic acid (pK_a= 3.75). Formic acid was used in place of the PMA, while maintaining all other components at the same concentration. This allowed pH 9.0 to be achieved and a similar ionic strength maintained in both methods, while providing for direct detection of UV active species. The use of a stabilizing agent (DTPA) and purging samples with nitrogen was performed to minimize analyte degradation, as the sulfide and thiosalt species are easily oxidized by impurities and air.[21,22,23,24] The optimized methods exhibited excellent linearities, detection limits and reproducibility. The CZE methods were successfully applied to the analysis of charged sulfur species including sulfate (SO_4^{2-}), thiosulfate ($S_2O_3^{2-}$), tetrathionate ($S_4O_6^{2-}$), sulfite (SO_3^{2-}), and bisulfide (HS^-) in

reservoir samples. The application of the methods developed in this project solved the challenges presented by the high chloride concentration in the produced water (Chapter 2).

There were many challenges encountered during the indirect CZE-UV-Vis method development; these are reported in Chapters 3 and 4. First and foremost, interconversion occurs spontaneously between various sulfur-containing species, with rates and pathways depending on the particular conditions such as pH and the relative nucleophilicity of sulfur oxyanions. For example, tetrathionate will react with sulfite to form thiosulfate and trithionate, and it can also decompose to trithionate and pentathionate. Bisulfide will also react with sulfite to produce thiosulfate. Meanwhile, thiosulfate can be hydrolyzed to sulfate and bisulfide. According to this study as well as previous studies, multiple reaction pathways have been proposed in the reactivity of thiosulfate, sulfate, bisulfide anion, tetrathionate, and sulfite as described in Chapter 3. Oxidation of some sulfur species was another obstacle in this study. During CE operation, hydrogen and oxygen gases are generated by water electrolysis. These gases can block the connection between a solution and electrode or be entrained into the capillary. Naturally, oxygen gas is also an oxidizing agent that is active on sulfide, thiosulfate and polythionate, producing a mix of products were illustrated in Chapter 4.

5.2 Future Research

Based on the success of the CZE methods developed in this study and their suitability with respect to speed, sensitivity and robustness for use in a wide range of context, the opportunities for future applications of this approach are abundant. In the immediate

future, it will be important to apply the method to other complex produced water systems. CZE methods frequently suffer in the presence of high chloride concentrations. Similar to challenges confronted in this project, the interference of chloride with thiosulfate detection has been encountered by Chen et al.(2003) in analysis of wastewater.[6] The direct method will be a great solution to the analysis of other briny real samples in addition to overcoming other non-absorbing anion interference.

Future researchers may also consider optimizing the choice of detection wavelength used with the PMA chromophoric probe, which could improve detection sensitivity for some sulfur containing anions that absorb in the same region as trimellitate (λ_{max} 254 nm).[6]

Using a stabilizing agent (DTPA), purging the water with nitrogen, and replenishing the BGE minimizes the presence of oxygen and keeps BGE composition consistent, making the method suitable for use with reactive species that are sensitive to condition changes. These very stable conditions provide a means to carry our further studies on a broader range of sulfur species while ensuring a lower probability for uncontrolled redox reactions.

According to the literature, there are some side reactions that may occur in a mixtures of sulfur compounds, resulting in the formation of other sulfur species such as polythionates (e. g., trithionate, pentathionate), polysulfides, and inorganic zero valent sulfur. This can impact the mass balance calculation. For future work, researchers should consider the analysis of these compounds by using the optimized CZE methods to completely determine how the mass has been distributed in the mixture of sulfur species.

Such work will be key to developing a clear understanding of the mechanisms of transformation and impacts of sulfur species on reservoir souring.

5.3 References

(1) Okoro, C.; Smith, S.; Chiejina, L.; Lumactud, R.; An, D.; Park, H. S.; Voordouw, J.; Lomans, B. P.; Voordouw, G. *J. Ind. Microbiol. Biotechnol.* **2014**, *41* (4), 665–678.

(2) El-hady, D. A. *Journal of Analytical Chemistry* **2009**, *64* (11), 1166–1173.

(3) Clark, P. D.; Hyne, J. B.; David Tyrer, J. *Fuel* **1984**, *63* (1), 125–128.

(4) Holubnyak, Y.; Bremer, J. M.; Hamling, J. A.; Huffman, B. L.; Mibeck, B.; Klapperich, R. J.; Smith, S. A.; Sorensen, J. A.; Harju, J. A. In *SPE International Symposium on Oilfield Chemistry*; *Society of Petroleum Engineer*s **2011**.

(5) Marcano, N. *Geoscience engineering* **2013**, 2–5.

(6) Chen, Z.; Naidu, R. *Int. J. Environ. Anal. Chem.* **2003**, *83* (9), 749–759.

(7) O'Reilly, J. W.; Dicinoski, G. W.; Shaw, M. J.; Haddad, P. R. *Anal. Chim. Acta* **2001**, *432* (2), 165–192.

(8) Padarauskas, A.; Paliulionyte, V.; Ragauskas, R.; Dikcius, A. *J. Chromatogr. A* **2000**, *879* (2), 235–243.

(9) Divjak, B.; Goessler, W. *J. Chromatogr. A* **1999**, *844* (1–2), 161–169.

(10) Haddad, P. R.; Doble, P.; Macka, M. *Journal of chromatography* **1999**, *856*, 145–177.

(11) Haddad, P. R. *J. Chromatogr. A* **1997**, *770* (1–2), 281–290.

(12) Chen, M. L.; Ye, M. L.; Zeng, X. L.; Fan, Y. C.; Yan, Z. *Chinese Chem. Lett.* **2009**, *20* (10), 1241–1244.

(13) Motellier, S.; Descostes, M. *J. Chromatogr. A* **2001**, *907* (1–2), 329–335.

(14) Safizadeh, F.; Larachi, F. *Instrum. Sci. Technol.* **2014**, *42* (3), 215–229.

(15) Hissner, F.; Mattusch, J.; Heinig, K. *J. Chromatogr. A* **1999**, *848* (1–2), 503–513.

(16) Buszewski, B.; Dziubakiewicz, E.; Szumski, M. *Electromigration Techniques*; **2013**, 105, 203-210.

(17) Kellogg, W. W.; Cadle, R. D.; Allen, E. R.; Lazrus, A. L.; Martell, E. A. *Science* **1972**, *175* (4022), 587–596.

(18) Jarczynska, M.; Trojanowciz, M.; Pobozy, E. *Chromatographia* **2002**, 56, 723–728.

(19) Pappoe, M.; Bottaro, C. S. *Anal. Methods* **2014**, *6* (23), 9305–9312.

(20) De Carvalho, L. M.; Schwedt, G. *J. Chromatogr. A* **2005**, *1099* (1–2), 185–190.

(21) Petre, C. F.; Larachi, F. *J. Sep. Sci.* **2006**, *29*, 144–152.

(22) Hughes, M. N.; Centelles, M. N.; Moore, K. P. *Free Radic. Biol. Med.* **2009**, *47* (10), 1346–1353.

(23) Zhang, H.; Jeffrey, M. I. *Inorg. Chem.* **2010**, *49* (22), 10273–10282.

(24) Laine, P.; Matilainen, R. *Anal. Bioanal. Chem.* **2005**, *382* (7), 1601–1609.